

Who Should Get Vaccinated? Individualized Allocation of Vaccines Over SIR Network

Toru Kitagawa[†] and Guanyi Wang[‡]

May 27, 2022

Abstract

How to allocate vaccines over heterogeneous individuals is one of the important policy decisions in pandemic times. This paper develops a procedure to estimate an individualized vaccine allocation policy under limited supply, exploiting social network data containing individual demographic characteristics and health status. We model spillover effects of the vaccines based on a Heterogeneous-Interacted-SIR network model and estimate an individualized vaccine allocation policy by maximizing an estimated social welfare (public health) criterion incorporating the spillovers. While this optimization problem is generally an *NP-hard* integer optimization problem, we show that the SIR structure leads to a submodular objective function, and provide a computationally attractive greedy algorithm for approximating a solution that has theoretical performance guarantee. Moreover, we characterise a finite sample welfare regret bound and examine how its uniform convergence rate depends on the complexity and riskiness of social network. In the simulation, we illustrate the importance of considering spillovers by comparing our method with targeting without network information.

Keywords: Vaccine allocation, Statistical treatment choice, Submodularity, SIR model, Social network, Spillovers.

[†]Department of Economics, University College London. Email: t.kitagawa@ucl.ac.uk

[‡]Department of Economics, University College London. Email: guanyi.wang.17@ucl.ac.uk
We would like to thank Andrew Chesher, Raffaella Giacomini, Aureo de Paula, Martin Weidner and the participants at 2020 UCL Economics department upgrade seminar. We thank Jeff Rowley for excellent research assistance.

1 Introduction

Allocation of a resource over individuals who interact within a social network is an important task in many fields, such as economics, medicine, education, and engineering. Learning an ideal treatment allocation rule under network interference is important in many applications in economics. One notable example is targeted investigation of suspected criminals who are connected within a social network. Given a limit budget, it is crucial to identify the “key players” in the network, as an effective means of reducing delinquency and crime (Lee et al., 2020). “Brute force” policy ¹ without proper targeting could incur cost to the society especially when resources are scarce. The several COVID-19 vaccines, which are currently in progress for potentially saving millions of lives, are one such scarce resource.

Since there are already ten COVID-19 vaccines in Phase 3 clinical trials (WHO et al., 2020a), an optimal evidence-based vaccine allocation proposal is urgently demanded by WHO and governments (WHO et al., 2020b). Globally, WHO has suggested using population proportional allocation, which means 3% of the population of each country would initially receive the vaccine, and that allocation would continue until each country has 20% vaccinated population (WHO et al., 2020c). However, there is a natural question: How to distribute vaccines optimally to individuals in every country? Answering that question raises many complex problems relating to public health, economics, inequality, and other considerations. Since most recent works target country level vaccine distribution, there is still no clear individualized vaccine assignment rule that has been adopted.

What is the purpose of vaccine allocation? To cut transmission of the virus. As such, policymakers need to consider spillover effects during vaccine allocation. Since the start of the current pandemic, governments around the world have gone to great lengths to collect network data in which one can trace who is contacting whom. It is reasonable to conclude that policymakers have already noticed the importance of network data. Without taking into account network effects, risk can only be evaluated based on individual covariates, such as age, area, or race. The implication is that younger individuals with numerous infected neighbors will not receive the vaccine. The estimated distribution rule must be biased in that case. We illustrate this point in our simulation exercises. Our proposed allocation policy improves the average probability of individuals staying healthy by 5% ~

¹Brute force means the government has zero tolerance for any crime.

12% compared with an allocation policy that ignores spillover effects, and this range of improvement is insensitive to the aspects of simulation design including the variation of SIR parameters and the size and density of network.

To formulate the spread of an infectious disease, one widely used epidemiological model is the *Susceptible-Infectious-Recovered* (SIR) model. This model has been adopted for measuring the flow patterns between each compartment since the early 20th century. Encouraged by [Acemoglu et al. \(2020\)](#), we provide a *Heterogeneous-Interacted-SIR* (HI-SIR) model to capture the spillover from each unit. Based on that model, we are able to measure the personal risk of being infected through their network. We recognize that it is not the first time a heterogeneous SIR model (e.g. [Chen et al. 2020](#)) has been used to analyze the vaccine allocation rule. However, where this model has been used, heterogeneity has often been measured at the group level, and personal interaction is commonly ignored in the allocation analysis.

Motivated by these considerations, we study how to choose the optimal vaccine assignment under capacity constraint. We use observational network data to do this. Data is informative about the covariates of N units, their health status, and their associated neighbors. Using in-sample information, we evaluate the risk, calculated from its own covariates and spillovers from the heterogeneous neighbors, to each unit using an *individualized Susceptible-Infectious-Recovered* model. The purpose of vaccine allocation is to maximize public health, by selecting units to be vaccinated. Obtaining an optimal assignment is, however, challenging since what treatment is optimal for one individual depends on what treatments are given to her neighbors. This implies that the search for an optimal allocation has to be performed over the entire network jointly, not individually.

This paper makes two main contributions. The first contribution is to develop methods to learn vaccine assignment policies that exploit network information at the micro-level. The second contribution is to show that the empirical welfare criterion built upon the SIR spillover structure delivers a submodular objective function and we can exploit it to obtain computationally attractive algorithms to solve the welfare optimization. Distinct from the existing approach of estimating individualized allocation policies under network interference ([Viviano, 2019](#); [Ananth, 2020](#)), our setting does not assume the availability of Randomized Control Trial (RCT) data. Instead, we assume the availability of estimated values of these spillover parameters from other sources, which we plug into our SIR model (e.g. [Ellison \(2020\)](#)). The advantage of not relying on RCT data is that the planner does

not need to run an RCT, which could be costly in terms of time and other resources when the policy action needs to be urgent. Exploiting already estimated SIR parameters allows for immediate targeting and allocation.

To optimize the empirical welfare in allocation policies, one naive approach is brute-force that evaluates the value of empirical welfare exhaustively for all the possible combinations of vaccine allocations over the individuals. Although the brute-force approach is guaranteed to optimize the empirical welfare globally, it is not practicable since the number of possible combinations grows exponentially as the number of individuals in the network increases. On the other hand, giving up the optimization entirely and implementing random allocation is indeed practicable, but leads to a significant waste of the vaccine supply, which we show in our simulation exercises.

Given the challenge in optimizing the empirical welfare, what we recommend in this paper is an allocation policy obtained by greedy optimization. A greedy optimization algorithm in the current setting is to sequentially allocate a vaccine to an individual in the network who is most influential for improving the social welfare. In general, greedy algorithms are not guaranteed to yield a global optimum. With the current welfare criterion built upon the SIR spillover structure, however, we can characterize a performance guarantee of the greedy-algorithm based allocation policy in terms of the welfare regret. To obtain it, we formulate the welfare optimization problem as a *quadratic integer programming (QIP)* problem. We show that this QIP problem features a submodular objective function regardless of the parameter values of the SIR structure we impose for the spillovers. Relying on the seminal result in discrete convex analysis shown by [Nemhauser et al. \(1978\)](#), we show that the greedy algorithm delivers an allocation policy at which the value of the objective function is worse than the global optimum only up to a universal constant factor. Our derivation of the population welfare regret of the greedily estimated allocation policy reflects the potential loss of welfare due to non-feasibility of obtaining the brute-force allocation policy. To our knowledge, this paper is the first to show and exploit submodularity of the empirical welfare function for learning individualized treatment allocation policy in the presence of spillovers.

We further illustrate the advantages of our method in our simulation exercises. In a small network setting (up to 35 individuals in the network), comparisons with the brute-force allocation rules reveal that our proposed greedy allocation rules leads to a global optimum solution. In a large network setting, we evaluate the performance of our method

versus with two different assignment rules, random assignment and targeting without considering network information. The welfare improvement relative to these two baselines ranges over 5% - 12%, and this result is insensitive to the values of SIR parameters and the size and density of network.

As considered by many policymakers and researchers, after the health situation has been brought under control, other aims (e.g. restoration of economic and social activities) should be used to evaluate the vaccine allocation rule (WHO et al., 2020b; Emanuel et al., 2020). These outcome variables can be handled in our framework. Our method can accommodate other exogenous constraints including a capacity constraint on each demographic group defined by observable covariates, e.g., the policymaker wants to limit the number of vaccines for those who can work at home.

We show optimality of our vaccine allocation rule in terms of the convergence rate, which measures how quickly the expected public health obtained from employing the estimated vaccine distribution rule converges to the first best public health condition. There is considerable uncertainty surrounding the value of the SIR parameters in the case of COVID-19 (Manski and Molinari, 2020). The optimal vaccine allocation policy is sensitive to these values, which is illustrated by the results of our simulation exercises. We choose regret to evaluate the performance of our proposed algorithm, since it can help us to understand the theoretical gap between our policy to the truly optimal assignment rule no matter the value of estimated SIR parameters and the distribution of random sample. Under a weak condition, the uniform upper bound of regret depends upon two things. Firstly, n , which is the sample size of the separate dataset used to estimate the SIR parameters. Secondly, the ratio of the network data sample size N to the maximum number of neighbors N_M plus the minimum between the number of infected units N_I and the number of available vaccines d (i.e. $(3dN_M + \min\{N_I, d\})/N$). As N_E and N_I grow, the complexity and risk of the social network increase, which reduces the efficiency and performance of the vaccine allocation rule.

The remainder of this paper is organized as follows. We first discuss the relevant literature in the rest of this section. Section 2 details the model, and the Heterogeneous-Interacted SIR model in particular, and the wider setting. Section 3 is concerned with estimation, including the estimation of SIR parameters and the construction of the QIP problem. The optimization procedure is contained in section 4. Section 5 contains the theoretical results. Simulation details are shown in section 6. Section 7 discusses some

potential extensions and Section 8 concludes. All proofs and derivations are shown in the appendix.

1.1 Related Literature

Our work contributes to the literature on statistical treatment rules, which was first introduced into econometrics by [Manski \(2004\)](#). The optimal treatment allocation regime has been studied in many fields, such as medical statistics ([Zhao et al., 2012, 2015](#)), operational research ([Loiola et al., 2007](#)) and economics. In econometrics and machine learning, researchers normally use regret to evaluate the performance of decision rules, and in recent years, this literature has grown rapidly. It includes [Dehejia \(2005\)](#), [Hirano and Porter \(2009\)](#), [Stoye \(2009, 2012\)](#), [Tetenov \(2012\)](#), [Kitagawa and Tetenov \(2018\)](#), [Mbakop and Tabord-Meehan \(2016\)](#), [Zhou et al. \(2018\)](#), [Manski \(2019\)](#), [Kasy and Sautmann \(2019\)](#), [Sakaguchi \(2019\)](#), [Athey and Wager \(2020\)](#), and [Kock et al. \(2020\)](#) among others. The planner’s objective function in the majority of these works is a sum of individual outcomes under the no-interference assumption (i.e. Stable Unit Treatment Value Assumption of [Rubin \(1974\)](#)). This assumption does not hold in this study, because of the network spillover effects. To our knowledge, there have been two papers that also consider the network setting in statistical treatment choice, [Viviano \(2019\)](#) and [Ananth \(2020\)](#). These two papers assume availability of pilot data from RCT studies performed over networks in order to form empirical welfare criteria. Their frameworks are not restricted to the SIR setting of the current paper and cover spillover structures commonly assumed in social science applications. In contrast, our approach forms welfare estimates by imposing the HI-SIR model structure and plugging in values of the primitive spillover parameters estimated or calibrated in some external study (e.g. [Baqae et al. \(2020\)](#)). Another notable difference is that we consider allocation policies that are not constrained other than the capacity constraint, while [Viviano \(2019\)](#) and [Ananth \(2020\)](#) assume the class of implementable allocation policies has a finite VC-dimension to control overfitting to the training RCT sample.

The SIR model was originally proposed by [Kermack and McKendrick \(1927\)](#), and is now the workhorse model in the epidemiological literature. Many extended versions have been studied in epidemiological analyses, such as the Susceptible-Infected-Susceptible model ([Nåsell, 1996](#)) and the Susceptible-Exposed-Infected-Recovered model ([Li and Mul-](#)

downey, 1995). During the global pandemic, an epidemiological literature has sprung up within economics. Atkeson (2020) and Stock (2020) introduce the SIR model into economics to study the implications of the current pandemic on the US economy. We introduce heterogeneity into the SIR model, which is similar to what Acemoglu et al. (2020) in studying the Multi-Risk SIR model. However, that paper assumes the infection rate after the release of a vaccine equals zero, which means it does not consider the vaccine allocation problem. Our work contributes to the current literature by studying micro-level vaccine assignment rules in a heterogeneous SIR model with network information. Previous works in the epidemiological literature also consider spillover effects and network interference. Pastor-Satorras and Vespignani (2002) states that considering network information when designing a vaccination policy increases its effectiveness and decreases the risk of infectious disease. Bu et al. (2020) estimates the epidemic processes under a dynamic network setting. It is worth noting that vaccination policy in the epidemiological literature often focuses on solving for the optimal proportion of vaccinated units in the population. For instance, (Manski, 2010, 2017) provide suggestions on how to choose the proportion of vaccinated units, whereas we consider who is vaccinated.

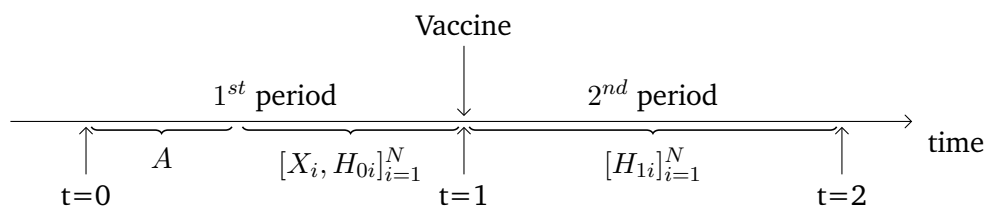
We build a connection to the literature on using a submodular function to solve an optimization problem. The performance guarantee of a general greedy algorithm for solving submodular maximization problem with a cardinality constraint was first introduced by Nemhauser et al. (1978). The later literature links the cardinality constraint to a more general constraint: Matroid constraint (Fisher et al., 1978; Cunningham, 1985). An overview of papers studying submodular functions is summarized in survey literature (Bach, 2011; Krause and Golovin, 2014). Recently, researchers have proposed high-speed greedy algorithms for the maximization problem (Mirzasoleiman et al., 2014; Balkanski et al., 2019). Integer optimizations of submodular functions appear in a wide variety of fields, such as electrical networks (Narayanan, 1997), graph theory (Frank, 1993), computer science (Krause and Guestrin, 2007), machine learning (Mirzasoleiman et al., 2013) and stochastic process theory (Macchi, 1975). In this work, we discuss a submodular function with a uniform matroid constraint (i.e. capacity constraint) and a more general partition matroid constraint.

We also note that there is a growing literature on the estimation of treatment effects under network interference. Manski (2013) discusses the identification of treatment effects and spillover effects under a deterministic interference graph and a set of relevant

potential outcomes. The increased number of network datasets that have recently become available has motivated further work on this topic, including [Sävje et al. \(2017\)](#), [Aronow et al. \(2017\)](#), [Athey et al. \(2018\)](#), [Basse et al. \(2019\)](#), and [Leung and Moon \(2019\)](#). [Li and Wager \(2020\)](#) non-parametrically estimates the direct effect and also the indirect effect of treatment in a random network setting. [Vazquez-Bare \(2020\)](#) describes the estimation of spillover effects using an instrument variable. We estimate the spillover effects by using epidemic model parameters. However, the aforementioned papers, which study the identification problem of network effects, could also be used to learn the optimal policy under a network setting.

2 Setup and Identification

We consider a basic model to study the vaccination allocation problem. Let us first introduce the timeline and data setting that we consider in this work.



As shown in this illustration, we suppose there are two periods. At $t = 0$, policymakers initially observe the network structure A among the individuals (i.e. adjacency matrix), for which we provide further details below. The policymakers then observe covariates $X_i \in \mathcal{X} \subset \mathbb{R}^{d_x}$ and current period health state $H_0 \in \{S, I, R\}$ for N units. The health states $\{S, I, R\}$ stand for *Susceptible*, *Infected*, and *Recovered*. We assume the network structure A is observed before personal health status to avoid the impact from self-isolation. At $t = 1$, policymakers start to assign the vaccine. After a short vaccine period, people begin to meet their neighbors, which we call the interaction period. The health state during that period is defined as $H_1 \in \{S, I, R, D\}$, where D stands for death. Since at the time of assigning vaccine, H_1 is not observed yet for researchers, a stochastic health state will be used to evaluate personal risk. The ultimate goal of policymakers is to maximize the expected social health situation via the allocation of vaccines.

In our setting, units are connected through a social network. We assume the following property on network structure holds:

Assumption 2.1. (*Undirected Relationships*) *The interference graph is undirected. i.e. $A_{ij} = A_{ji}$.*

The symmetric $N \times N$ adjacency matrix A represents the network, with the (i, j) th element of A , denoted by A_{ij} , equal to one if unit i and unit j are connected, and zero otherwise. By convention, all the diagonal elements A_{ii} are equal to zero. If $A_{ij} = 1$, then we say that i and j are neighbors. Let N_i indicate the neighbors of unit i , then we write $A_{ij} = 1$ if $j \in N_i$ and $i \in N_j$. The network structure is a fixed characteristic of the population.

Now, let us introduce the notation that we use in the following sections. First, v_i is the individual vaccine assignment rule (i.e. $v_i = 1$ if unit i gets the vaccine). Let \mathbf{v} denote $(v_1, \dots, v_N) \in \{0, 1\}^N$, and X denote $(X_1, \dots, X_N) \in \mathbb{R}^{N \times d_x}$. Let S_i be the susceptible state indicator in first period (i.e. $S_i = \mathbb{1}_{\{H_{0i}=S\}}$), let I_i be the infected state indicator in first period (i.e. $I_i = \mathbb{1}_{\{H_{0i}=I\}}$), and let R_i be the recovered state indicator in first period (i.e. $R_i = \mathbb{1}_{\{H_{0i}=R\}}$). Moreover, let $|N_i|$ denote the number of neighbors for unit i (i.e. $|N_i| = \sum_j A_{ij}$).

2.1 Heterogeneous-Interacted-SIR model

To measure the personalized transition probability, we use a **HI-SIR** model. Our model is defined in discrete time within a simplified setting of two time periods. In the first period, we observe the health state of each unit H_0 , which belongs to S (Susceptible), I (Infected), or R (Recovered),

$$S_i + I_i + R_i = 1. \quad (1)$$

In the second period, the state variable is H_1 . Compared with H_0 , H_1 includes one more state D (Death).

$$\mathbb{1}_{\{H_{1i}=S\}} + \mathbb{1}_{\{H_{1i}=I\}} + \mathbb{1}_{\{H_{1i}=R\}} + \mathbb{1}_{\{H_{1i}=D\}} = 1. \quad (2)$$

Without the vaccine, the state can move from susceptible to infected, then to either recovery or death. Now, we consider the setting after introducing the vaccine. Generally, vaccination has two purposes: the first is limiting the spread of disease, and the second is treatment. Vaccination builds up the immune system, which leads to recovery. However,

the effectiveness of vaccination (i.e. the percentage of vaccinated units that recover) is not clear. For simplicity, we assume that assumption 2.2 holds.

Assumption 2.2. (PT) *Perfect Treatment*: A vaccinated unit enters the Recovered state, regardless of its previous state (i.e. $\Pr(H_{1i} = R|v_i = 1) = 1$).

To further simplify the setting, we split all units into a finite number of disjoint groups based on their characteristics. The infection rate between each group varies. This setting could be extended to the individual level, but need to know the micro level infection rate. Here, we use **age** as the binary indicator and only consider two groups: G_1 (*Young*) and G_2 (*Old*). We now define a_i and b_i as the group indicator (i.e. $a_i = \mathbb{1}_{\{X_i \in G_1\}}$ and $b_i = \mathbb{1}_{\{X_i \in G_2\}}$).

We specify one of the key components in the SIR models, the infection rate of unit i , as:

$$q_i = \left[\beta_{11} \frac{\sum_{j \in N_i} I_j (1 - v_j) a_j}{|N_i|} + \beta_{12} \frac{\sum_{j \in N_i} I_j (1 - v_j) b_j}{|N_i|} \right] \cdot a_i + \left[\beta_{21} \frac{\sum_{j \in N_i} I_j (1 - v_j) a_j}{|N_i|} + \beta_{22} \frac{\sum_{j \in N_i} I_j (1 - v_j) b_j}{|N_i|} \right] \cdot b_i, \quad (3)$$

where $\beta_{sk} = -\kappa_s \log(1 - c_{sk})$, c_{sk} is the probability of successful disease transmission following a contact between group s and group k (i.e. c_{11} measures that transmission probability from one unit to another within the young group, c_{12} is the corresponding probability of transmission from a unit in the old group to a unit in the young group, with similar definitions for c_{21} and c_{22}), κ_s is the average number of contacts in group s at each time period. β_{sk} describes the effective contact rate of the disease between group s and group k . The derivation of equation 3 can be found in the appendix.

In the above expression, $I_j(1 - v_j)$ means susceptible individual can only be infected by neighbors who were infected and not vaccinated². Those neighbors may come from various groups. We calculate the fraction of neighbors in each group and multiply them by the associated risk parameters. The risk parameter β_{sk} measures the probability that susceptible individual in group i being infected from group s in one time period.

²This can also be thought of as an underlying assumption, which is commonly used in epidemiological literature (e.g. Pesaran and Yang (2020)).

We now define $\{\gamma_1, \gamma_2\}$ as the recovery rate and $\{\delta_1, \delta_2\}$ as the mortality in group 1 and group 2 respectively. Given that, we can formulate the probability of staying in the infection state for the infected unit i as:

$$p_i = 1 - a_i(\gamma_1 + \delta_1) - b_i(\gamma_2 + \delta_2). \quad (4)$$

Since the probability of recovery and death purely depend on personal physical fitness³, there is no interactive part in equation 4. The transition probability of being infected state is then:

$$P_{I_i}(\mathbf{v}) \equiv \Pr(H_{1i} = I|X, \mathbf{v}, A, H_0) = S_i q_i \cdot (1 - v_i) + I_i p_i \cdot (1 - v_i). \quad (5)$$

In the above expression, the probability of an unvaccinated unit being infected has two components. The first is the probability of a healthy unit being infected. The second is the probability of staying in the infected state for those infected in the first period. Under Assumption 2.2, a vaccinated unit has zero probability of being infected. Similarly, the probability of being susceptible is:

$$P_{S_i}(\mathbf{v}) \equiv \Pr(H_{1i} = S|X, \mathbf{v}, A, H_0) = [1 - v_i - q_i(1 - v_i)] \cdot S_i. \quad (6)$$

An unvaccinated unit can only exit the susceptible state by infection. Therefore, the probability of staying in state S decreases with the risk parameter β_{sk} , which depends on the number of infected neighbors and the number of contacts with them. The remaining two states do not rely on the network structure. First, the probability of recovery:

$$P_{R_i}(\mathbf{v}) \equiv \Pr(H_{1i} = R|X, \mathbf{v}, A, H_0) = v_i + [R_i + I_i(a_i\gamma_1 + b_i\gamma_2)] \cdot (1 - v_i). \quad (7)$$

In the above expression, recovery has two different sources. One is the vaccine, and the other is self-immunity. The effect of self-immunity is heterogeneous and varies with personal characteristics. The probability of building immunity in each group is γ_1, γ_2 . The last

³This can be thought as a simplified assumption, which indicates the death rate does not depend on the availability of hospital spare capacity.

state is death, which occurs with probability

$$P_{Di}(\mathbf{v}) \equiv \Pr(H_{1i} = D|X, \mathbf{v}, A, H_0) = I_i(a_i\delta_1 + b_i\delta_2) \cdot (1 - v_i). \quad (8)$$

2.2 Optimal Vaccine Allocation Problem

In Emanuel et al. (2020), a group of medical ethics experts suggest a successful vaccine is needed to reduce death and morbidity from infection, and is also needed for the restoration of economic and social activity. Following that suggestion, we choose our baseline outcome variable as the probability of being healthy in the second period. Alternatively, we can consider economic or some other public health purposes that can be formulated as a function of our discrete health status outcome variable (to be discussed in section 7). Equation (9) summarizes all the previous considerations and sets up the constrained optimization problem:

$$\max_{\mathbf{v} \in \{0,1\}^N} \frac{1}{N} \sum_{i=1}^N \sum_{h \in \{S,R\}} P_{hi}(\mathbf{v}), \quad (9)$$

s.t.

$$\sum_{i=1}^N v_i \leq d, \quad (10)$$

where

$$P_{hi}(\mathbf{v}) = \Pr(H_{1i} = h|X, \mathbf{v}, A, H_0), \quad (11)$$

and $d \geq 1$ is a positive integer for the exogenous cardinality constraint. The main idea of the above objective function is to maximize the average probability of being in the susceptible or recovered state in the second period by appropriately assigning the d units of vaccine.

In equation (9), P_{hi} is the heterogeneous state transition function, which describes the probability of $h \in \{S, R\}$ in the second period. This transition probability depends on the individual covariates, associated network structure, and their previous state. In this work, we adopt the HI-SIR model to formulate the above transition function, which has been provided in the last section.

One relevant question is: Will vaccine allocation change the network structure? Yes,

it will change the behaviour of vaccinated units. For example, vaccinated units prefer to go out as compared to unvaccinated units. In that case, the number of contacts at each time period κ_s and the network structure A will change after vaccination. It is certainly restrictive that our objective function keeps the network structure of period 2 being fixed at the one observed in period 1. If we want to relax this, we can incorporate probabilistic uncertainty for A in period 2, if any available, by taking the expectation of the objective function with respect to random adjacency matrices of period 2 conditional on \mathbf{v} . We, however, do not consider such extension in this paper and leave it for future research.

The following question is: Since the network structure changes after introducing the vaccination policy, will this variation have an impact on our problem? No, the reason being that we only study a one time period setting. We evaluate the probability of being in each health state in the second period, which means we ignore any network effects beyond the second period. However, this network variation should be considered if we look at multiple periods setting.

3 Estimation

In the last section, we formulated our problem using the **HI-SIR** model. In order to measure the individual risk level by using this epidemic model, we need to know the associated SIR parameters: transmission rate (i.e. $\beta_{11}, \beta_{12}, \beta_{21}, \beta_{22}$), and recovery rate (i.e. γ_1, γ_2). Given that we cannot observe the true value of those parameters, it is infeasible to evaluate the objective function (9) based on the in-sample information of (H_0, X) and A of the target network. We therefore assume access to a separate dataset with sample size n or an external study analyzing it. from which we can form estimates for these exogenous parameters. We construct an empirical version of the population welfare (9) and maximize over the feasible allocation policies. To reflect the precision of the SIR parameter estimates into the welfare performance of an estimated allocation rule, we explicitly take into account the sampling uncertainty of the parameter estimates in our derivation of the welfare regret upper bound.

3.1 Estimation of SIR Parameters

The estimation of infection rate and death rate always faces severe missing data problems as discussed in (Manski and Molinari, 2020). Keeling and Rohani (2011) points out that, usually, researchers first estimate the reproductive ratio \mathcal{R}_0 , which is the average number of individuals that one sick person infects.

$$\mathcal{R}_0 = \beta \times \frac{1}{\gamma}. \quad (12)$$

Then, the infection rate can be derived from the estimated recovery rate $\hat{\gamma}$ and $\hat{\mathcal{R}}_0$. In our case, the reproductive ratio is heterogeneous at group level.

$$\mathcal{R}_{0sk} = \beta_{sk} \times \frac{1}{\gamma_s} \quad \forall s, k = 1, 2, \quad (13)$$

where \mathcal{R}_{0sk} is the number of infectious individuals in group s resulting from one sick person in group k . We need to estimate the average number of young infectious and old infectious from one sick person in group 1 and group 2, and also the recovery rate in each group. Given these, we can estimate $\beta_{11}, \beta_{12}, \beta_{21}, \beta_{22}$ from equation 13.

Remark 3.1. We are not going to discuss what is the desirable procedure for estimating the model parameters in this work, since the choice of estimator depends on the type of data (e.g. Seroprevalence data, Reported cases data, etc.). For more reference, see Keeling and Rohani (2011). For Covid-19, the estimation of \mathcal{R}_0 and other SIR parameters has been done in several papers, including Fernández-Villaverde and Jones (2020) and Ferguson et al. (2020).

Plugging these estimates into our **HI-SIR** model, we now have the sample analogue of the population maximization problem (9), which is

$$\begin{aligned} \max_{\mathbf{v} \in \{0,1\}^N} W_n(\mathbf{v}), \quad \text{s.t.} \quad \sum_{i=1}^N v_i \leq d, \quad \text{where} \\ W_n(\mathbf{v}) = \frac{1}{N} \sum_{i=1}^N \sum_{h \in \{S,R\}} \hat{P}_{hi}(\mathbf{v}). \end{aligned} \quad (14)$$

3.2 Quadratic Integer Programming

To solve equation (14), we reformulate it as a quadratic integer programming (QIP) problem, which in the context of assignment problem over network is known as Quadratic Assignment Problem (QAP) of Koopmans and Beckmann (1957). QAP is a classical combinatorial optimization problem popular in the operational research literature.

$$W_n(\mathbf{v}) = \frac{1}{N} \sum_{i=1}^N v_i + \frac{1}{N} \sum_{i=1}^N \left[R_i + (a_i \hat{\gamma}_1 + b_i \hat{\gamma}_2) I_i \right] (1 - v_i) + \frac{1}{N} \sum_{i=1}^N \left[1 - M_i \right] S_i (1 - v_i) \quad (15)$$

s.t.

$$\sum_{i=1}^N v_i \leq d, \quad (16)$$

$$v_i \in \{0, 1\} \quad \forall i = 1, \dots, N, \quad (17)$$

where

$$M_i = \frac{\sum_{j=1}^N (\hat{\beta}_{11} a_i a_j + \hat{\beta}_{12} a_i b_j + \hat{\beta}_{21} b_i a_j + \hat{\beta}_{22} b_i b_j) A_{ij} I_j (1 - v_j)}{|N_i|}. \quad (18)$$

In equation (15), there are two linear terms and one quadratic term in \mathbf{v} . The first term measures the direct effect of vaccination. A vaccinated unit is safe from infection with 100% probability. The last two terms describe the probability of being free of infection for unvaccinated units. Infected units naturally recover with probability $\{\gamma_1, \gamma_2\}$, which depends on their own characteristics. For those units who are already recovered in the first period, they are free from infection in the second period. The last component takes into account the indirect effect of vaccination. For susceptible units, the probability of being infected by their infected neighbors is summarized by the interaction term.

After removing all the constant parts in equation (15), we obtain a simplified objective function (i.e. $W_n(\mathbf{v}) = F_n(\mathbf{v}) + \text{constant}$):

$$F_n(\mathbf{v}) = \frac{1}{N} \sum_{i=1}^N \hat{c}_i v_i + \frac{1}{N} \sum_{i=1}^N \frac{1}{|N_i|} \sum_{j=1}^N T_{ij} v_i + \frac{1}{N} \sum_{i=1}^N \frac{1}{|N_i|} \sum_{j=1}^N T_{ij} v_j - \frac{1}{N} \sum_{i=1}^N \frac{1}{|N_i|} \sum_{j=1}^N T_{ij} v_i v_j, \quad (19)$$

where

$$\hat{c}_i = 1 - R_i - (a_i\hat{\gamma}_1 + b_i\hat{\gamma}_2)I_i - S_i, \quad (20)$$

$$T_{ij} = (\hat{\beta}_{11}a_ia_j + \hat{\beta}_{12}a_ib_j + \hat{\beta}_{21}b_ia_j + \hat{\beta}_{22}b_ib_j)A_{ij}I_jS_i. \quad (21)$$

Since F_n differs from W_n only by an additive constant (conditional on the network structure and individual characteristics at perior 1), the solution of F_n is equivalent to the solution of the original empirical welfare function W_n . Therefore, from now on, we will focus on $F_n(\mathbf{v})$ as our new objective function. Within $F_n(\mathbf{v})$, there is a quadratic term plus linear components in \mathbf{v} . Current software is available to solve general QIP problems, such as CPLEX and Gurobi. However, both applications require a **symmetric weighting matrix**, which does not hold in our case. This asymmetric property comes from the infectious process, since disease can only be transmitted from infected units to susceptible units, but the reverse is not true. We discuss how to solve this QIP problem with showing and exploiting the submodular property of our objective function in the next section.

4 Optimization

4.1 Submodularity

We showed in the last section that we can formulate our objective function as QAP. This kind of problem is well known as an *NP-hard* and *NP-hard to approximate* problem (Cela, 2013). Usually, we cannot solve this type of problem in polynomial time, which is an issue in practice. However, we can in general link our problem to the submodular optimization problem. The benefit of submodularity is that there exists off-the-shelf algorithms that can solve the submodular minimization problem in exact polynomial time and *approximately* solve the submodular maximization problem with capacity constraint in polynomial time. The seminal result of Nemhauser et al. (1978) provides a universal bound for the quality of approximation as detailed below in Section 4.2.

Definition 4.1 (Submodular function). Let $\mathcal{N} = \{1, 2, \dots, N\}$. A real-valued set-function $F: 2^{\mathcal{N}} \rightarrow \mathbb{R}$ is submodular if and only if, for all subsets $A, B \subseteq \mathcal{N}$, we have: $F(A) + F(B) \geq F(A \cap B) + F(A \cup B)$.

In simple terms, submodularity describes the diminishing returns property. The marginal

increase in the average probability of being healthy decreases in the number of vaccinated units. This property is crucial for the maximization algorithm. For ease of exposition, we express the simplified empirical welfare F_n as a set function with argument $V \in 2^{\mathcal{N}}$, where the binary vector of vaccine allocation $\mathbf{v} \in \{0, 1\}^N$ and V correspond by $V = \{i \in \mathcal{N} : v_i = 1\}$:

$$F_n(V) = \mathbf{v}^\top \hat{W} \mathbf{v} + \hat{C}^\top \mathbf{v} - \mathbf{1}_{N \times 1}^\top \hat{W} \mathbf{v} - \mathbf{v}^\top \hat{W} \mathbf{1}_{N \times 1}, \quad (22)$$

where

$$\hat{C} = \begin{bmatrix} \frac{\hat{c}_1}{N} \\ \vdots \\ \frac{\hat{c}_N}{N} \end{bmatrix}, \quad \mathbf{1}_{N \times 1} = \begin{bmatrix} 1 \\ \vdots \\ 1 \end{bmatrix}, \quad \hat{W} = \begin{bmatrix} \hat{w}_{11} & \hat{w}_{12} & \cdots & \hat{w}_{1N} \\ \hat{w}_{21} & \hat{w}_{22} & \cdots & \hat{w}_{2N} \\ \vdots & \vdots & \ddots & \vdots \\ \hat{w}_{N1} & \hat{w}_{N2} & \cdots & \hat{w}_{NN} \end{bmatrix}, \quad (23)$$

$$\hat{w}_{ij} = -\frac{1}{N} \frac{1}{|N_i|} (\hat{\beta}_{11} a_i S_i A_{ij} a_j I_j + \hat{\beta}_{12} a_i S_i A_{ij} b_j I_j + \hat{\beta}_{21} b_i S_i A_{ij} a_j I_j + \hat{\beta}_{22} b_i S_i A_{ij} b_j I_j). \quad (24)$$

We then denote the class of feasible allocation set V subject to cardinality constraint $|V| \leq d$ by $\mathcal{V}_d \equiv \{V \in 2^{\mathcal{N}} : |V| \leq d\}$. Since vaccinating additional individuals never harm the welfare, F_n is a *non-decreasing* set function, i.e., for any $V \subset V'$, $F_n(V) \leq F_n(V')$.

The quadratic functional form of F_n shown in (22) can be linked to one classic submodular function called as a *cut function*. Cut functions have been well studied in combinatorial optimization and graph theory. We apply some of the results from that literature (e.g. [Bach \(2011\)](#)).

Lemma 4.1. *Let $\hat{W} \in \mathbb{R}^{N \times N}$ and $\hat{C} \in \mathbb{R}^N$. Then the set function $F_n: V \mapsto \mathbf{v}^\top \hat{W} \mathbf{v} + \hat{C}^\top \mathbf{v} - \mathbf{1}_{N \times 1}^\top \hat{W} \mathbf{v} - \mathbf{v}^\top \hat{W} \mathbf{1}_{N \times 1}$ is submodular if and only if $\hat{w}_{ij} \leq 0 \forall i \neq j$.*

The proof is shown in the appendix. Note that the necessary and sufficient condition for submodularity shown in this lemma is distinct from the negative semidefiniteness of matrix \hat{W} . Since all the parameters in \hat{w}_{ij} are non-negative, we must have $\hat{w}_{ij} \leq 0, \forall i, j = 1, \dots, N$. This immediately leads to the following theorem:

Theorem 4.1. *The objective function $F_n(V)$ is a non-decreasing submodular function for any adjacency matrix, covariate values, and values of parameter estimates.*

Theorem 4.1 is the key result in our paper. It describes two important properties of our objective function; monotonicity and submodularity. We exploit these two properties to justify uses of greedy maximization algorithms shown in the next subsection.

4.2 Greedy Maximization Algorithm

Greedy maximization algorithms for submodular functions have been studied and frequently used for well over forty years. The performance guarantee of this algorithm was first introduced by Nemhauser et al. (1978). This algorithm essentially uses the diminishing returns property of the submodular function. The idea is to iteratively select the most valuable element until the capacity constraint is reached. At each round, the algorithm evaluates $\mathcal{O}(N)$ functions to identify the marginal gain of each element. The number of rounds depends on the capacity constraint d . As a result, the computational complexity of the greedy algorithm is at the order of $\mathcal{O}(N \cdot d)$, well below the computational complexity of the brute-force search. Algorithm 1 presents the greedy maximization algorithm applied to the maximization of the empirical welfare (22).

Algorithm 1: Capacity Constrained Greedy Algorithm

1: **Input:** Dataset $\{S_i, I_i, R_i, a_i, b_i\}_{i=1}^N, \{A_{ij}\}_{i,j=1}^N$, estimated parameters $\{\hat{\beta}_{11}, \hat{\beta}_{12}, \hat{\beta}_{21}, \hat{\beta}_{22}, \hat{\gamma}_1, \hat{\gamma}_2\}$, and capacity constraint d ;

2: **Initialization:** Starting from the empty set $V = \emptyset$;

if $|V| < d$ **then**

3: **for** each $i \in \mathcal{N} \setminus V$ **do**

4: Compute the marginal gain $F_n(V + \{i\}) - F_n(V)$;

5: Select i which maximizes the marginal gain and add it into the set V ;

else

return the set V ;

end

In general, there is no performance guarantee of the greedy algorithm. However, as shown by [Nemhauser et al. \(1978\)](#) for a non-decreasing submodular function with cardinality constraint (i.e. capacity constraint in our case), the greedy maximization algorithm is guaranteed to yield an allocation rule $\hat{V} \in \mathcal{V}_d$ that satisfies $F_n(\hat{V}) \geq (1 - \alpha_d)F_n(\hat{V}^*)$, where $\hat{V}^* \in \mathcal{V}_d$ is a constrained optimum under the capacity constraint which can be uncovered by the brute-force search, and α_d is a positive constant that depends only on $d \geq 1$ and $\alpha_d \geq 1/e$ for all $d \geq 1$. This seminal result implies that the greedy maximization algorithm provides a universal optimization guarantee for non-decreasing submodular function, $F_n(\hat{V}) \geq (1 - 1/e)F_n(\hat{V}^*) \approx 0.63F_n(\hat{V}^*)$. Since we show in [Theorem 4.1](#) that our objective function is non-decreasing and submodular, we obtain the following theorem as an immediate corollary of our [Theorem 4.1](#) and [Nemhauser et al. \(1978\)](#).

Theorem 4.2 ([Nemhauser et al. 1978](#)). *Let $F_n : 2^{\mathcal{N}} \rightarrow \mathbb{R}$ be the simplified empirical welfare function as defined in [\(22\)](#) and $\hat{V}^* \in \arg \max_{V \in \mathcal{V}_d} F_n(V)$, $d \geq 1$. The greedy algorithm shown in [Algorithm 1](#) outputs $\hat{V} \in \mathcal{V}_d$ such that*

$$F_n(\hat{V}) \geq (1 - \alpha_d)F_n(\hat{V}^*) \geq (1 - 1/e)F_n(\hat{V}^*), \quad (25)$$

where $\alpha_d \equiv \left(1 - \frac{1}{d}\right)^d$ is monotonically decreasing in d and converges to e^{-1} as $d \rightarrow \infty$.

4.3 Targeting Constraint

Up until now, we have only considered a simple capacity constraint in the vaccine assignment rule. In reality, policymakers may limit the number of vaccines that are administered in each group.⁴ For example,

- Policymakers may limit access to vaccines for those people that can work at home. If we are able to divide individuals into two groups based on their job categories, into a group that can work at home and a group that cannot say. Then, policymakers can set an upper bound on the number of vaccines that are available for the work at home group.

⁴A group in this section does not need to coincide with the group defining the heterogeneity of the SIR parameters. For example, we could divide units based on their job category, geographical location, or community.

- Policymakers may want to make a certain number of vaccines available for younger people due to their value in the labor force, and thereby, limit the number of vaccines that are available for older people. Without constraint, the algorithm might assign a large number of vaccines to the old group, which may be incompatible the target of the policymaker.

We call this kind of constraint a *targeting constraint*, since this constraint mainly depends on the target of policymakers. In this section, we consider the second example, which divides units based on their age. In this case, we can still use the notation that we define in the previous section. This constraint can be written as:

$$\sum_{i: X_i \in G_1} v_i = \sum_{i=1}^N a_i v_i \leq d_1, \quad \sum_{i: X_i \in G_2} v_i = \sum_{i=1}^N b_i v_i \leq d_2. \quad (26)$$

This targeting constraint belongs to a general class of constraints so called *matroid*. First, we use \mathcal{I} to describe the subset of $2^{\mathcal{N}}$ that is compatible with all of the constraints imposed. If we restrict the set of vaccinated agents V to belong to \mathcal{I} , which is part of a matroid $(\mathcal{Y}, \mathcal{I})$, this constraint is called a matroid constraint.

Definition 4.2 (Matroid). Let \mathcal{I} be a nonempty family of allowable subsets of \mathcal{N} . Then the tuple $(\mathcal{N}, \mathcal{I})$ is a matroid if it satisfies:

- (Hereditiy) For any $D \subset E \subset \mathcal{N}$, if $E \in \mathcal{I}$, then $D \in \mathcal{I}$.
- (Augmentation) For any $D, E \in \mathcal{I}$, if $|D| < |E|$, then there exists an $x \in E \setminus D$ such that $D \cup \{x\} \in \mathcal{I}$.

Let \mathcal{N}_1 and \mathcal{N}_2 be the disjoint subsets partitioned by X_i ($\mathcal{N}_1 \cup \mathcal{N}_2 = \mathcal{N}$). We can represent the targeting constraint by

$$\mathcal{I} \equiv \{V: V \subseteq \mathcal{N}, |V \cap \mathcal{N}_1| \leq d_1, |V \cap \mathcal{N}_2| \leq d_2\}. \quad (27)$$

We can show that this $(\mathcal{N}, \mathcal{I})$ is a matroid referred to as a *partition matroid*. First look at the hereditiy. For any $D \subset E$, we must have $|D \cap \mathcal{N}_1| \leq |E \cap \mathcal{N}_1|$ and $|D \cap \mathcal{N}_2| \leq |E \cap \mathcal{N}_2|$. If $E \in \mathcal{I}$, then it means D must satisfy the targeting constraint in \mathcal{I} . Next, for any $D, E \in \mathcal{I}$, we must have $|D \cap \mathcal{N}_1|, |E \cap \mathcal{N}_1| \leq d_1$ and $|D \cap \mathcal{N}_2|, |E \cap \mathcal{N}_2| \leq d_2$. If $|D| < |E|$, then either

$|D \cap \mathcal{N}_1| < |E \cap \mathcal{N}_1|$ or $|D \cap \mathcal{N}_2| < |E \cap \mathcal{N}_2|$ or both. As a result, there must exist an element x that belongs to $E \setminus D$ such that $|D \cup \{x\} \cap \mathcal{N}_1| \leq d_1$ and $|D \cup \{x\} \cap \mathcal{N}_2| \leq d_2$.

This problem of optimal treatment assignment subject to a partition matroid constraint is to maximize $F_n(V)$ over $V \in \mathcal{I}$. The following Algorithm 2 is guaranteed to produce a solution $\hat{V}' \in \mathcal{I}$.

Algorithm 2: Targeting Constraint Greedy Algorithm

1: **Input:** Dataset $\{S_i, I_i, R_i, a_i, b_i\}_{i=1}^N, \{A_{ij}\}_{i,j=1}^N$, estimated parameters $\{\hat{\beta}_{11}, \hat{\beta}_{12}, \hat{\beta}_{21}, \hat{\beta}_{22}, \hat{\gamma}_1, \hat{\gamma}_2\}$, capacity constraint d , and targeting constraints d_1, d_2 ;

2: **Initialization:** Starting from the empty set $V = \emptyset$;

if $|V| < d$ **then**

3: **for each** $i \in \mathcal{N} \setminus V$ **do**

4: Compute the marginal gain $F_n(V + \{i\}) - F_n(V)$;

5: Sort i in order of decreasing marginal gain

6. **if** $\sum_{j \in V} a_j + a_{i(1)} \leq d_1 \cup \sum_{j \in V} b_j + b_{i(1)} \leq d_2$ **then**

7: Add the 1st element of i into V ;

else

8: Repeat step 6 with remaining i ;

end

else

return the set V ;

end

Greedy maximization algorithms subject to the partitioned matroid constraint performed for non-decreasing submodular functions attain at least 50% of the optimal welfare.

Proposition 4.1 (Fisher et al. 1978). *Let $F_n : 2^{\mathcal{N}} \rightarrow \mathbb{R}$ be the simplified empirical welfare function as defined in (22) and $\hat{V}^{**} \in \arg \max_{V \in \mathcal{I}} F_n(V)$. The greedy maximization algorithm shown in Algorithm 2 outputs $\hat{V}' \in \mathcal{I}$ such that*

$$F_n(\hat{V}') \geq \frac{1}{2}F_n(\hat{V}^{**}). \quad (28)$$

The performance guarantee of the greedy algorithm with targeting constraint is worse than the performance guarantee of Algorithm 1. This implies a trade-off between additional constraints and the accuracy of computation. In the next section, we discuss the welfare regret bounds of the allocation rules estimated by the above greedy algorithms.

5 Regret Bounds

Following [Manski \(2004\)](#) and the subsequent literature on statistical treatment rules, we use regret to evaluate the performance of our algorithm on vaccine allocation. Let $F : 2^{\mathcal{N}} \rightarrow \mathbb{R}$ be the population analogue of $F_n(\cdot)$ in (22), where the estimated parameters are replaced by the truth. The expected regret measures the average difference in the welfare between using the constrained optimal assignment rule $V^* \in \arg \max_{V \in \mathcal{V}_d} F(V)$ and using the constrained estimated greedy algorithm \hat{V} obtained from Algorithm 1:

$$F(V^*) - \mathbb{E}_{P^n} [F(\hat{V})] = \mathbb{E}_{P^n} [F(V^*) - F(\hat{V})] \geq 0, \quad (29)$$

where \mathbb{E}_{P^n} is the expectation with respect to the sampling uncertainty of the parameter estimators in the external studies.

In this work, we assume that the consistent estimators of effective contact rate and recovery rate are available from other studies. Generally, there is no requirement on the estimator except that Assumption 5.1 needs to hold.

Assumption 5.1. *Let $\hat{\beta}_{sk}$ denote the estimate of effective contact rate between group s and group k , and $\hat{\gamma}_s$ denote the estimate of recovery rate in group s . The following properties need to hold:*

$$\mathbb{P} \left\{ \left| \hat{\beta}_{sk} - \beta_{sk} \right| \geq \epsilon \right\} \leq 2e^{-2n\epsilon^2} \quad \forall s, k = 1, 2. \quad (30)$$

$$\mathbb{P} \left\{ \left| \hat{\gamma}_s - \gamma_s \right| \geq \epsilon \right\} \leq 2e^{-2n\epsilon^2} \quad \forall s = 1, 2, \quad (31)$$

where \mathbb{P} is the sampling distribution in other study that has sample size n .

The above assumption is an exponential tail bound obtained by applying Hoeffding's large deviation inequality. Since β_{sk} is the effective contact rate of the disease between group s and k , and γ_s is the recovery rate in group s , they are naturally bounded in $[0, 1]$. Hence, common estimators (e.g. sample analogue) meet the above condition. However, other tail bounds might apply for some other estimators, which do not necessarily have the same form as the above tail bound. Our approach can accommodate various tail bounds, such as the tail bound associated with the maximum likelihood estimator (Miao, 2010).

The estimators for the contact rates and recovery rates may come from different studies with different sample sizes. In this case, we can view n in Assumption 5.1 as the smallest sample size among the studies.

In order to derive the uniform convergence rate of the welfare regret, we decompose regret into three components as follows.

$$F(V^*) - F(\hat{V}) = \underbrace{F(V^*) - F_n(\hat{V}^*)}_{\textcircled{1}} + \underbrace{F_n(\hat{V}^*) - F_n(\hat{V})}_{\textcircled{2}} + \underbrace{F_n(\hat{V}) - F(\hat{V})}_{\textcircled{3}}, \quad (32)$$

where V^* is an oracle optimum $V^* = \arg \max_{V \in \mathcal{V}_d} F(V)$, \hat{V}^* is a constrained optimal solution to the estimated welfare $\hat{V}^* = \arg \max_{V \in \mathcal{V}_d} F_n(V)$, and \hat{V} is the output from the greedy maximization algorithm under the capacity constraint. Therefore, $\textcircled{1}$ describes the regret we would attain if the constrained optimum could be computed exactly. $\textcircled{2}$ measures the welfare loss introduced by the greedy algorithm. $\textcircled{3}$ indicates the loss from using the estimated objective function instead of the true objective function. We compute the upper bound of each component separately and then combine them together.

First, we start from the derivation of the upper bound of $\textcircled{1}$. This part is similar to the approach in Kitagawa and Tetenov (2018). Before looking at V^* , consider the following inequality, which holds for any $\tilde{V} \in \mathcal{V}_d$:

$$\begin{aligned} F(\tilde{V}) - F_n(\hat{V}^*) &\leq F(\tilde{V}) - F_n(\tilde{V}) \\ &\quad (\because F_n(\hat{V}^*) \geq F_n(\tilde{V})) \\ &\leq \sup_{V \in \mathcal{V}_d} |F_n(V) - F(V)|. \end{aligned} \quad (33)$$

Since it applies to $F(\tilde{V})$ for all \tilde{V} , it also applies to V^* :

$$F(V^*) - F_n(\hat{V}^*) \leq \sup_{V \in \mathcal{V}_d} |F_n(V) - F(V)|. \quad (34)$$

For the second component, we can obtain an upper bound by applying Theorem 4.2:

$$\begin{aligned} F_n(\hat{V}^*) - F_n(\hat{V}) &\leq \frac{1}{e} F_n(\hat{V}^*) \\ &\leq \frac{1}{e} (F_n(\hat{V}^*) - F(\hat{V}^*)) + \frac{1}{e} F(V^*) \\ &\leq \frac{1}{e} |F_n(\hat{V}^*) - F(\hat{V}^*)| + \frac{1}{e} F(V^*) \\ &\leq \frac{1}{e} \sup_{V \in \mathcal{V}_d} |F_n(V) - F(V)| + \frac{1}{e} F(V^*). \end{aligned} \quad (35)$$

Similarly to the first component, the third component can be bounded as:

$$F_n(\hat{V}) - F(\hat{V}) \leq |F_n(\hat{V}) - F(\hat{V})| \leq \sup_{V \in \mathcal{V}_d} |F_n(V) - F(V)|. \quad (36)$$

Combining all the previous results, we obtain the upper bound of regret:

$$F(V^*) - F(\hat{V}) \leq \left(2 + \frac{1}{e}\right) \sup_{V \in \mathcal{V}_d} |F_n(V) - F(V)| + \frac{1}{e} F(V^*). \quad (37)$$

Compared with the regret upper bound when one could compute \hat{V}^* , the regret upper bound shown in (37) has one additional term $\frac{1}{e} \sup_{V \in \mathcal{V}_d} |F_n(V) - F(V)| + \frac{1}{e} F(V^*)$. This additional term comes from equation (35) and captures the welfare loss induced by the use of greedy algorithm. As we characterize below, the first term converges to zero as $n \rightarrow \infty$ under Assumption 5.1, while the second term remains independent of accuracy of the parameter estimates. A simulation study of Section 6 assesses the magnitude of the optimization error of the greedy algorithm, and show numerically that the greedy algorithm yields an exact optimum at least for small network cases ($N = 35$). Based on this, we believe that the optimization error term of the greedy algorithm is much smaller than the universal theoretical bound $\frac{1}{e} F(V^*)$.

In the partition matroid (targeting constraint) case, by applying Proposition 4.1 and repeating the arguments to derive (37), we obtain

$$F(V^{**}) - F(\hat{V}') \leq \frac{5}{2} \sup_{V \in \mathcal{I}} |F_n(V) - F(V)| + \frac{1}{2} F(V^{**}), \quad (38)$$

where V^{**} is an oracle optimum under the targeting constraint, $V^{**} \in \arg \max_{V \in \mathcal{I}} F(V)$.

In order to bound $\sup_{V \in \mathcal{V}_d} |F_n(V) - F(V)|$, we use the triangle inequality to find the bound of $|F_n(V) - F(V)|$:

$$\begin{aligned} |F_n(V) - F(V)| &= \left| \mathbf{v}^\top (\hat{W} - W) \mathbf{v} + (\hat{C}^\top - C^\top) \mathbf{v} - \mathbf{1}_{N \times 1}^\top (\hat{W} - W) \mathbf{v} - \mathbf{v}^\top (\hat{W} - W) \mathbf{1}_{N \times 1} \right| \\ &\leq \left| \mathbf{v}^\top (\hat{W} - W) \mathbf{v} \right| + \left| (\hat{C}^\top - C^\top) \mathbf{v} \right| + \left| \mathbf{1}_{N \times 1}^\top (\hat{W} - W) \mathbf{v} \right| + \left| \mathbf{v}^\top (\hat{W} - W) \mathbf{1}_{N \times 1} \right| \\ &\leq \mathbf{v}^\top |\hat{W} - W| \mathbf{v} + |(\hat{C}^\top - C^\top)| \mathbf{v} + \mathbf{1}_{N \times 1}^\top |\hat{W} - W| \mathbf{v} + \mathbf{v}^\top |\hat{W} - W| \mathbf{1}_{N \times 1}, \end{aligned} \quad (39)$$

where the absolute value of a matrix or vector stands for the element-wise absolute values. Therefore, we can decompose the maximal deviation $\sup_{V \in \mathcal{V}} |F_n(V) - F(V)|$ into four parts:

$$\begin{aligned} \sup_{V \in \mathcal{V}_d} |F_n(V) - F(V)| &\leq \sup_{V \in \mathcal{V}_d} \mathbf{v}^\top |\hat{W} - W| \mathbf{v} + \sup_{V \in \mathcal{V}_d} |\hat{C}^\top - C^\top| \mathbf{v} \\ &\quad + \sup_{V \in \mathcal{V}_d} \mathbf{1}_{N \times 1}^\top |\hat{W} - W| \mathbf{v} + \sup_{V \in \mathcal{V}_d} \mathbf{v}^\top |\hat{W} - W| \mathbf{1}_{N \times 1}. \end{aligned} \quad (40)$$

Under Assumption 5.1, we can obtain an upper bound for the mean for each element in $\hat{W} - W$ and $\hat{C} - C$, as shown in the next lemma.

Lemma 5.1. *Under Assumptions 2.1, 2.2, and 5.1, we have*

$$\mathbb{E}_{P^n} |\hat{w}_{ij} - w_{ij}| \leq \sqrt{\frac{1 + \log(2)}{2n}} \frac{A_{ij}}{N}, \quad \mathbb{E}_{P^n} |\hat{c}_i - c_i| \leq \sqrt{\frac{1 + \log(2)}{2n}} \frac{I_i}{N}. \quad (41)$$

Combining this lemma with equations (40) and (37), we obtain the following theorem:

Theorem 5.1. *Let $N_M = \max_{i \in \mathcal{N}} |N_i|$, and N_I be the total number of infected units. Under Assumptions 2.1, 2.2, and 5.1, we have*

$$\mathbb{E}_{P^n} [F(V^*) - F(\hat{V})] \leq \bar{C} \cdot \frac{3dN_M + \min\{N_I, d\}}{N} \sqrt{\frac{1}{n}} + \frac{1}{e} F(V^*), \quad (42)$$

where \bar{C} is a universal constant and d is the number of available vaccines.

Proof of the above theorem is shown in the Appendix. In Theorem 5.1, we provided a distribution-free upper bound on the expected regret. We show that the convergence rate of the upper bound depends on the network data sample size N and also the sample size n for estimating the SIR parameters. At the same time, the regret upper bound is increasing in the complexity and the riskiness of the network and the number of available vaccines. The intuition is that our algorithm becomes harder to identify the most valuable units when the maximum number of edges and the number of infected individuals in the network increases. Moreover, our algorithm becomes harder to identify the best allocation rule when the number of possible combinations increase, which is introduced by relaxing the capacity constraint. This also implies the benefit of quarantine. Since quarantine controls the maximum number of connections in the network, the effectiveness of vaccine allocation is boosted by such government policy. Therefore, there is advantage to complementing a vaccine assignment policy with quarantine, which is evidenced by our simulation exercises.

6 Simulation Exercises

In this section, we use an Erdős-Renyi graph to generate a random social network. In each of the following tables, we use twenty different networks and take the average of the outcome variable across all of the networks. We choose the probability of allocating a unit to group 1 to be 40% and the probability of allocating a unit to group 2 to be 60% (i.e. $\mathbb{P}(X_i = G_1) = 0.4$ and $\mathbb{P}(X_i = G_2) = 0.6$). In the epidemiological literature, researchers usually find the steady state of the SIR parameters. In order to identify the impact of varying the SIR parameters, we choose two different sets of parameter values to run the simulation. Throughout our simulation studies, we do not consider sampling errors in the parameter estimates and focus on optimising welfare with true parameter values plugged in. Table 1 summarizes all the values of the SIR parameters that we have used.

In addition, we choose three different numbers of edges, $7N$, $10N$ and *full*, in order to identify the effect of network complexity. Here, *full* means that the network is fully connected (i.e. complete graph). We choose *full* to understand the behaviour of our heuristic algorithm not only in the sparse network case but also in the densest case. We also compare three capacity constraints, $d = 7\%N, 10\%N, 20\%N$, to evaluate the marginal performance gain of our greedy algorithm.

<i>Parameters</i>	<i>set 1</i>	<i>set 2</i>	<i>Parameters</i>	<i>set 1</i>	<i>set 2</i>
β_{11}	0.7	0.8	β_{12}	0.5	0.5
β_{21}	0.5	0.7	β_{22}	0.6	0.7
γ_1	0.1	0.1	γ_2	0.05	0.025

Table 1: Summary of the SIR parameter values

In the following sections, we compare our greedy algorithm with three familiar allocation rules. We first compare our algorithm with a brute force method in order to find the difference between the potentially sub-optimal greedy solution and the brute-force optimal solution. However, the number of possible combinations dramatically increases with the number of nodes and the capacity constraint. We cannot use a large number of agents to compute the brute force optimum in the simulation. Given this, in section 6.2, we use a random assignment rule as a baseline to evaluate the performance of our algorithm in a large network setting. The third allocation rule that we compare our greedy algorithm with is an allocation rule which assigns the vaccine without considering network information. We compare the greedy algorithm with that third rule in section 6.3.

6.1 Comparing with Brute Force

Since Theorem 4.2 shows the gap between the optimal solution and the heuristic result is at most 37%, we want to explore that theoretical difference using numerical study. We list all the possible combinations and use brute force to search for the optimal solution given a manageable number of units. We specify the maximum number of units to be $N = 35$, which is limited by computer performance. As the number of nodes increases, the possible number of combinations grows exponentially. The memory requirement and running time become impractical in a more realistic case. We recognize that the results from a small network may not be accurate in a large network setting, but it may help us to understand the regret of our greedy algorithm to some degree. We summarize the in-sample welfare W_n of these two approaches in table 2.

<i>Allocation Rule</i>	<i>Greedy Algorithm</i>			<i>Brute Force</i> ⁵		
	<i>d = 7%N</i>	<i>d = 10%N</i>	<i>d = 20%N</i>	<i>d = 7%N</i>	<i>d = 10%N</i>	<i>d = 20%N</i>
Parameter set 1						
<i>N = 30, edges = 7N</i>	0.47	0.51	0.63	0.47	0.51	0.63
<i>N = 30, edges = 10N</i>	0.41	0.45	0.57	0.41	0.45	0.57
<i>N = 30, edges = Full</i>	0.31	0.35	0.47	0.31	0.35	0.47
<i>N = 35, edges = 7N</i>	0.47	0.55	0.65	0.47	0.55	0.65
<i>N = 35, edges = 10N</i>	0.42	0.49	0.59	0.42	0.49	0.59
<i>N = 35, edges = Full</i>	0.29	0.36	0.46	0.29	0.36	0.46
Parameter set 2						
<i>N = 30, edges = 7N</i>	0.45	0.49	0.62	0.45	0.49	0.62
<i>N = 30, edges = 10N</i>	0.38	0.43	0.55	0.38	0.43	0.55
<i>N = 30, edges = Full</i>	0.27	0.32	0.44	0.27	0.32	0.44
<i>N = 35, edges = 7N</i>	0.46	0.54	0.65	0.46	0.54	0.65
<i>N = 35, edges = 10N</i>	0.40	0.48	0.59	0.40	0.48	0.59
<i>N = 35, edges = Full</i>	0.26	0.33	0.44	0.26	0.33	0.44

Table 2: Comparing the probability of being healthy in second period between Greedy Algorithm and Brute Force

In the small network case, we find that our greedy algorithm finds the global optimum in all cases that we consider, which indicates a good performance of our method. We also notice that the welfare that is associated with the global optimum decreases with the number of edges. As we relax the capacity constraint, welfare increases rapidly. The main purpose of this comparison is to get an idea on how much the empirical welfare at the greedy solution can be worse than the brute force optimum. More results are illustrated in the following two sections.

⁵We compare all the possible combinations given the capacity constraint and select the set V that maximizes W_n .

6.2 Comparing With Random Assignment

In this section, we use a random assignment rule to define the baseline of vaccine allocation. We randomly draw an allocation 10,000 times and calculate the average value of the outcome variable. Random allocation is one common assignment rule for policymakers. The purpose of this simulation is to learn the improvement of our greedy allocation rule. In order to evaluate its performance in a relatively large network setting, we choose $N = 500$ and 800. Table 3 records the main differences in terms of in-sample welfare between these two methods.

<i>Allocation Rule</i>	<i>Greedy Algorithm</i>			<i>Random Assignment</i> ⁶		
	$d = 7\%N$	$d = 10\%N$	$d = 20\%N$	$d = 7\%N$	$d = 10\%N$	$d = 20\%N$
Parameter set 1						
$N = 500, edges = 7N$	0.61	0.65	0.77	0.57	0.59	0.65
$N = 500, edges = 10N$	0.60	0.64	0.76	0.56	0.58	0.65
$N = 500, edges = Full$	0.33	0.36	0.48	0.29	0.31	0.38
$N = 800, edges = 7N$	0.62	0.66	0.78	0.58	0.60	0.66
$N = 800, edges = 10N$	0.61	0.65	0.77	0.57	0.59	0.66
$N = 800, edges = Full$	0.15	0.18	0.30	0.11	0.13	0.20
Parameter set 2						
$N = 500, edges = 7N$	0.60	0.64	0.77	0.55	0.58	0.65
$N = 500, edges = 10N$	0.59	0.63	0.76	0.55	0.57	0.64
$N = 500, edges = Full$	0.25	0.28	0.41	0.21	0.24	0.31
$N = 800, edges = 7N$	0.62	0.66	0.79	0.57	0.59	0.66
$N = 800, edges = 10N$	0.61	0.65	0.77	0.56	0.59	0.66
$N = 800, edges = Full$	0.09	0.13	0.25	0.06	0.08	0.15

Table 3: Comparing the probability of being healthy in second period between Greedy Algorithm and Random allocation

⁶We randomly select an assignment 10,000 times and take the average value of the outcome variable.

From table 3, we find that the performance of both methods decreases with the number of edges, which is the same case for the first comparison. As the number of edges increase, the greedy algorithm finds it harder to identify who is relatively crucial in the network, which supports our theorem in the previous section. This effect becomes more pronounced as the capacity constraint is relaxed. In the most extreme case, when everyone is connected with each other, the performance of our method is still better than the random assignment rule. This performance gap widens with the capacity constraint. We also find that the average welfare increases by 12% when the capacity constraint increases by $0.1N$. The number of nodes increases the performance of our method in a sparse network setting. However, welfare in the densest network is comparatively low, approximately 18% for parameter set 1 and 15% for parameter set 2, no matter which capacity constraint we use. Moreover, the effect of varying the SIR parameter values on welfare is more pronounced when the random assignment rule is used.

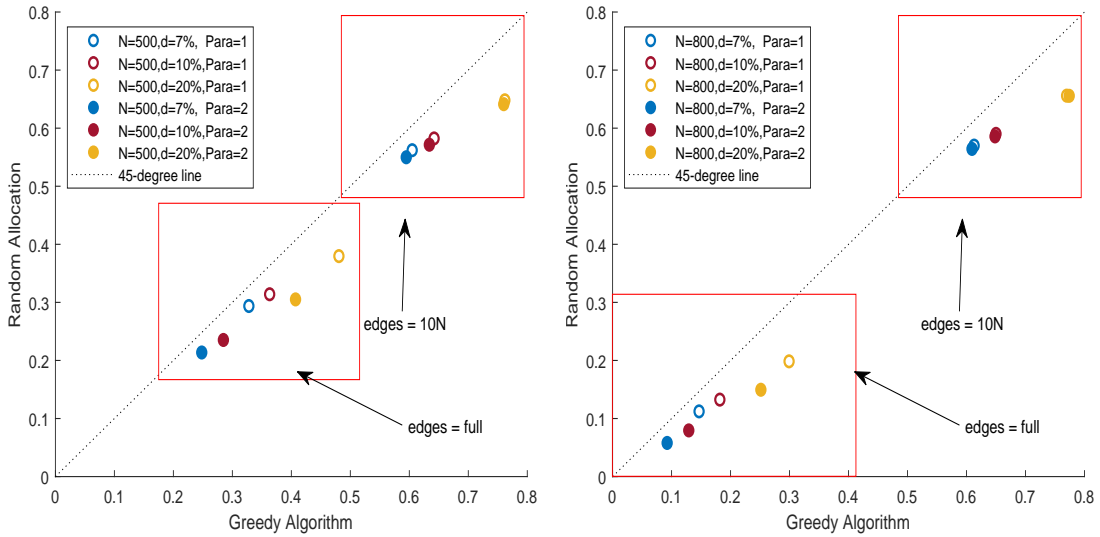


Figure 1: Comparison between Greedy Algorithm and Random allocation

If we look at the random assignment rule, its performance is much worse than the performance of the greedy algorithm. This difference increases when the complexity of and the number of nodes in the network increase. The performance of the random assignment rule improves as we relax the capacity constraint. However, this improvement is only about 7% when the capacity constraint increases by $0.1N$. Compared with the greedy algorithm,

random assignment is less effective. Given the shortage of vaccine, we waste considerable resources by randomly assigning the vaccine. Looking at the situation of full edges, the performance of random allocation is inferior. The ratio of the welfare attained by the random allocation to the welfare attained by the greedy algorithm is illustrated in figure 1. This ratio increases slowly with the number of edges and decreases with the number of nodes in the network. In addition, the ratio decreases in an obvious way with the number of vaccines that are available.

6.3 Comparing With Targeting Without Network Information

<i>Allocation Rule</i>	<i>Greedy Algorithm</i>			<i>Group 2 Assignment⁷</i>		
	$d = 7\%N$	$d = 10\%N$	$d = 20\%N$	$d = 7\%N$	$d = 10\%N$	$d = 20\%N$
Parameter set 1						
$N = 500, edges = 7N$	0.61	0.65	0.77	0.57	0.59	0.66
$N = 500, edges = 10N$	0.60	0.64	0.76	0.57	0.59	0.66
$N = 500, edges = Full$	0.33	0.36	0.48	0.30	0.32	0.39
$N = 800, edges = 7N$	0.62	0.66	0.78	0.58	0.60	0.66
$N = 800, edges = 10N$	0.61	0.65	0.77	0.57	0.59	0.66
$N = 800, edges = Full$	0.15	0.18	0.30	0.11	0.14	0.20
Parameter set 2						
$N = 500, edges = 7N$	0.60	0.64	0.77	0.56	0.58	0.65
$N = 500, edges = 10N$	0.59	0.63	0.76	0.56	0.58	0.65
$N = 500, edges = Full$	0.25	0.28	0.41	0.22	0.24	0.31
$N = 800, edges = 7N$	0.62	0.66	0.79	0.58	0.60	0.66
$N = 800, edges = 10N$	0.61	0.65	0.77	0.57	0.59	0.66
$N = 800, edges = Full$	0.09	0.13	0.25	0.06	0.08	0.15

Table 4: Comparing the probability of being healthy in second period between Greedy Algorithm and Targeting Without Network Information

⁷We assign the vaccine only to the second group (i.e. only older people receive the vaccine).

Usually, in the literature of treatment assignment, researchers use observational data or experimental data without network structure information to study the optimal policy. As a result, the allocation regime assigns the treatment without considering spillover effects, which could lead to sub-optimal result. We call this kind of regime Targeting Without Network Information (TWNI). In this simulation, we want to learn the welfare loss from using TWNI versus our method.

Generally, TWNI assigns treatment based on personal characteristics. In this study, we only have one covariate: *age*. That means either the old group receives the vaccine or the young group receives the vaccine. Under the previous setting (i.e. older people are more likely to be infected and to die), group 2 will consume the entire vaccine allocation. Therefore, we call this regime *Group 2 Assignment*. Given different capacity constraints, this assignment rule selects units to be vaccinated from group 2 until the upper bound is reached. The above table indicates our main finding from our simulation exercises.

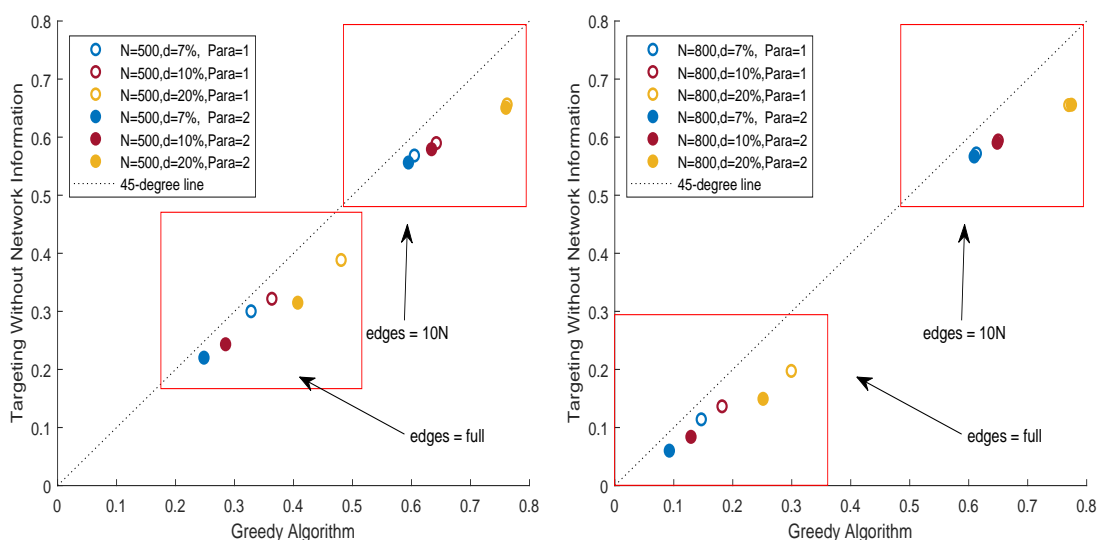


Figure 2: Comparison between Greedy Algorithm and Targeting Without Network Information

As shown in table 4, the results for TWNI allocation are similar to those for random allocation. The performance gap between TWNI and our greedy method increases with the number of allowable vaccines. We notice the gap decreases slightly with the number of edges, which means the performance of TWNI is better than random allocation when the

network is denser. These results are also illustrated in figure 3. By comparing the results for a different number of nodes, we find that the performance of both methods improves with the size of the population. However, that property only holds in the sparse network setting, which also includes the random assignment rule. In addition, despite the outcome value varying with the SIR parameters, the sizable improvement from using network information to allocate vaccination is quite robust to variations in the size and density of network.

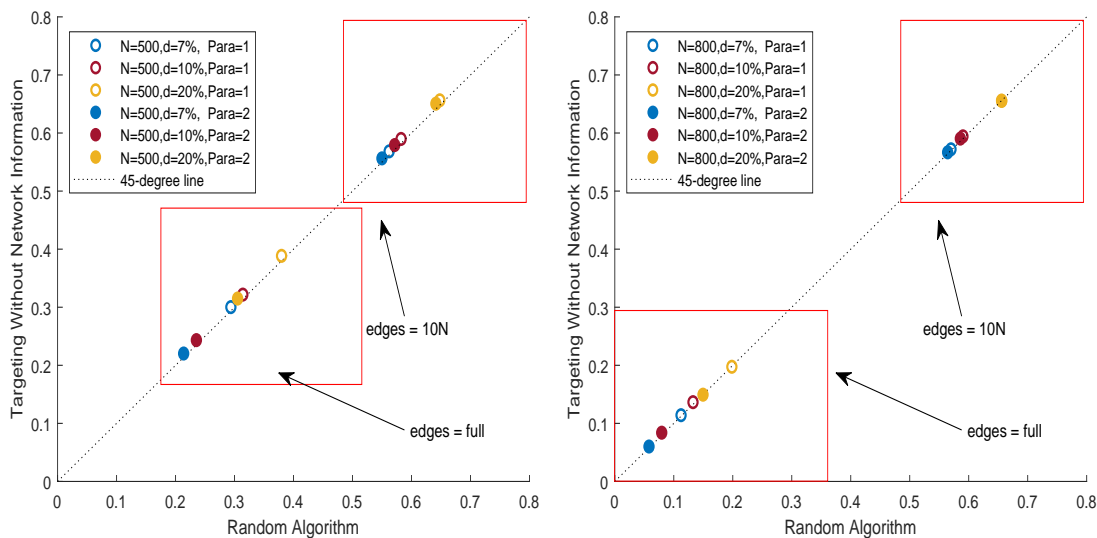


Figure 3: Comparison between Random allocation and Targeting Without Network Information

Based on the above results, we observe that if the number of available vaccines is small, the loss from ignoring network information is relatively small (around 4%). However, this loss increases dramatically with the number of available vaccines. In addition, the performance gap between our greedy algorithm and the other two allocation methods decreases with the network complexity (i.e. the number of edges). Under what might be described as a lockdown policy, the density of the network is maintained at a relatively low level, which raises the cost of ignoring spillovers. This cost also increases with the number of units in the population, which is a problem in a more realistic setting. We further show that the performance improvement from considering network information is robust to variation of the SIR parameters, which suggests that our conclusion is irrelevant to the parameters that we choose in the simulation. As a result, the allocation rule which

ignores the spillovers waste a sizeable proportion of a scarce resource.

7 Extensions

7.1 General Outcome Variable

In the previous sections, we only consider the health index as the outcome variable. However, in the real case, the policymakers may have different targets, and these targets could depend on individual level health index, as well as occupation, age, or some other personal characteristics. In that case, our problem becomes :

$$\max_{\mathbf{v} \in \mathcal{V}_d} \frac{1}{N} \sum_{i=1}^N \sum_{h \in H_1} P_{hi}(\mathbf{v}) \mathbb{E}[Y_{i1}|h, X_i], \quad (43)$$

where $\mathbb{E}[Y_{i1}|h, X_i]$ is the expected outcome variable conditional on the predicted second period health state, and personal covariates. Based on the above expression, policymakers can target different objects. For example, if policymakers want to revive the economy, the consumption level or the labor supply could be used as the outcome variable. The individual consumption level potentially depends on an individual's own health situation and personal characteristics, which could be formulated by $\mathbb{E}[C_{i1}|H_1, X_i]$. It can be shown, with the new outcome variable, that submodularity still holds. That means greedy maximization algorithms similar to Algorithms 1 and 2 shown above can apply and be expected to perform well. Moreover, the regret bound can be shown to be similar to the bound in Theorem 5.1 but will further depend on additional constants that would appear in the large deviation inequalities of Assumption 5.1 if the parameters are estimated from non-binary outcome observations.

7.2 Perfect Treatment Assumption and Submodularity

Recall Assumption 2.2 (Perfect Treatment): A vaccinated unit enters the Recovered state, regardless of its previous state (i.e. $\Pr(H_{1i} = R|v_i = 1) = 1$). There are three possible ways to relax this assumption :

- The recovered units can still spread disease.

- The recovered units will become susceptible after one period (few periods).
- Some percentage of vaccinated units remain susceptible or infected.

In the first case, if the person is recovered at H_0 , he will spread the disease during the first period. In that case, the recovered neighbors of unit i will be taken into account by the infection rate q_i . However, that will not change the sign of our weighting matrix, hence submodularity (by Theorem 4.1). In the second case, if unit i is recovered in the first period (i.e. $H_{0i} = R$), he could become susceptible in the second period (i.e. $H_{1i} = S$). Then, he may be infected in the next period (i.e. $H_{2i} = I$). However, we only consider a one time period setting in this work, which rules this risk out. In the third case, varying this percentage only affects the coefficient of the linear term in the objective function (i.e. \hat{c}_i in equation 19), which is irrelevant to submodularity.

8 Conclusion

In this work, we have introduced a novel method to estimate individualized vaccine allocation rules under network interference. We introduce the heterogeneous-interacted-SIR model to specify the spillover effects of infectious disease. We show that the welfare objective function of the vaccine allocation problem is non-decreasing and submodular, and so is its empirical analogue formed by plugging in the estimates of the SIR parameters. Based on this specific diminishing returns property, we provide a greedy algorithm with performance guarantee under two different exogenous constraints, which can easily accommodate various targets that policymakers commonly face in reality. Moreover, we show that this algorithm implies an upper bound for regret that converges uniformly at $\mathcal{O}(n^{-1/2})$. Using simulation, we point out the importance of considering network information in the allocation problem.

Several open questions and extensions are worth considering in future works. First, this paper considered a one-time vaccine allocation. We did not consider if there are multiple allocation periods, and how to decide the allocation dynamically. Moreover, we do not study how the vaccine allocation rule impacts on the outcome variables after multiple periods. As discussed in Bu et al. (2020), changes to the network structure should be considered in a dynamic setting. Second, we only compare the greedy algorithm with the

brute force optimum in a small network. Other than the universal bounds of Theorem 5.1, we do not know the performance of our method relative to the optimal solution in the large network data setting. Third, we assume the SIR parameters are estimated from separate observational data. It is an open question how to use the clinical trial data of a COVID-19 vaccine to estimate the treatment effect. Fourth, we did not impose any other constraints than the capacity constraint and the targeting constraint. For interpretability and fairness, we may want to additionally restrict the policy rule as a simple function of observed covariates. We regard these as interesting questions that are worthy of consideration.

References

- Acemoglu, D., Chernozhukov, V., Werning, I., and Whinston, M. D. (2020). A multi-risk sir model with optimally targeted lockdown. Technical report, National Bureau of Economic Research.
- Ananth, A. (2020). Optimal treatment assignment rules on networked populations. *working paper*.
- Aronow, P. M., Samii, C., et al. (2017). Estimating average causal effects under general interference, with application to a social network experiment. *The Annals of Applied Statistics*, 11(4):1912–1947.
- Athey, S., Eckles, D., and Imbens, G. W. (2018). Exact p-values for network interference. *Journal of the American Statistical Association*, 113(521):230–240.
- Athey, S. and Wager, S. (2020). Policy learning with observational data. *Econometrica*.
- Atkeson, A. (2020). What will be the economic impact of covid-19 in the us? rough estimates of disease scenarios. Technical report, National Bureau of Economic Research.
- Bach, F. (2011). Learning with submodular functions: A convex optimization perspective. *arXiv preprint arXiv:1111.6453*.
- Balkanski, E., Rubinstein, A., and Singer, Y. (2019). An exponential speedup in parallel running time for submodular maximization without loss in approximation. In *Proceedings*

- of the *Thirtieth Annual ACM-SIAM Symposium on Discrete Algorithms*, pages 283–302. SIAM.
- Baqae, D., Farhi, E., Mina, M. J., and Stock, J. H. (2020). Reopening scenarios. Technical report, National Bureau of Economic Research.
- Basse, G., Feller, A., and Toulis, P. (2019). Randomization tests of causal effects under interference. *Biometrika*, 106(2):487–494.
- Bellstedt, M. and Dathe, H. (1992). The cone of nondecreasing set functions. In *Operations Research'91*, pages 131–133. Springer.
- Bu, F., Aiello, A. E., Xu, J., and Volfovsky, A. (2020). Likelihood-based inference for partially observed epidemics on dynamic networks. *Journal of the American Statistical Association*, pages 1–17.
- Cela, E. (2013). *The quadratic assignment problem: theory and algorithms*, volume 1. Springer Science & Business Media.
- Chen, X., Li, M., Simchi-Levi, D., and Zhao, T. (2020). Allocation of covid-19 vaccines under limited supply. Available at SSRN 3678986.
- Cunningham, W. H. (1985). Minimum cuts, modular functions, and matroid polyhedra. *Networks*, 15(2):205–215.
- Dehejia, R. H. (2005). Program evaluation as a decision problem. *Journal of Econometrics*, 125(1-2):141–173.
- Ellison, G. (2020). Implications of heterogeneous sir models for analyses of covid-19. Technical report, National Bureau of Economic Research.
- Emanuel, E. J., Persad, G., Kern, A., Buchanan, A., Fabre, C., Halliday, D., Heath, J., Herzog, L., Leland, R., Lemango, E. T., et al. (2020). An ethical framework for global vaccine allocation. *Science*, 369(6509):1309–1312.
- Ferguson, N., Laydon, D., Nedjati-Gilani, G., Imai, N., Ainslie, K., Baguelin, M., Bhatia, S., Boonyasiri, A., Cucunubá, Z., Cuomo-Dannenburg, G., et al. (2020). Report 9: Impact

- of non-pharmaceutical interventions (npis) to reduce covid19 mortality and healthcare demand. *Imperial College London*, 10:77482.
- Fernández-Villaverde, J. and Jones, C. I. (2020). Estimating and simulating a sird model of covid-19 for many countries, states, and cities. Technical report, National Bureau of Economic Research.
- Fisher, M. L., Nemhauser, G. L., and Wolsey, L. A. (1978). An analysis of approximations for maximizing submodular set functions—ii. In *Polyhedral combinatorics*, pages 73–87. Springer.
- Frank, A. (1993). Submodular functions in graph theory. *Discrete Mathematics*, 111(1-3):231–243.
- Hirano, K. and Porter, J. R. (2009). Asymptotics for statistical treatment rules. *Econometrica*, 77(5):1683–1701.
- Hoeffding, W. (1994). Probability inequalities for sums of bounded random variables. In *The Collected Works of Wassily Hoeffding*, pages 409–426. Springer.
- Kasy, M. and Sautmann, A. (2019). Adaptive treatment assignment in experiments for policy choice. *CESifo Working Paper*.
- Keeling, M. J. and Rohani, P. (2011). *Modeling infectious diseases in humans and animals*. Princeton University Press.
- Kermack, W. O. and McKendrick, A. G. (1927). A contribution to the mathematical theory of epidemics. *Proceedings of the royal society of london. Series A, Containing papers of a mathematical and physical character*, 115(772):700–721.
- Kitagawa, T. and Tetenov, A. (2018). Who should be treated? empirical welfare maximization methods for treatment choice. *Econometrica*, 86(2):591–616.
- Kock, A. B., Preinerstorfer, D., and Veliyev, B. (2020). Functional sequential treatment allocation. *Journal of the American Statistical Association*, pages 1–36.
- Koopmans, T. C. and Beckmann, M. (1957). Assignment problems and the location of economic activities. *Econometrica: journal of the Econometric Society*, pages 53–76.

- Krause, A. and Golovin, D. (2014). Submodular function maximization.
- Krause, A. and Guestrin, C. (2007). Near-optimal observation selection using submodular functions. In *AAAI*, volume 7, pages 1650–1654.
- Lee, L.-F., Liu, X., Patacchini, E., and Zenou, Y. (2020). Who is the key player? a network analysis of juvenile delinquency. *Journal of Business & Economic Statistics*, pages 1–9.
- Leung, M. P. and Moon, H. R. (2019). Normal approximation in large network models. Available at SSRN 3377709.
- Li, M. Y. and Muldowney, J. S. (1995). Global stability for the seir model in epidemiology. *Mathematical biosciences*, 125(2):155–164.
- Li, S. and Wager, S. (2020). Random graph asymptotics for treatment effect estimation under network interference. *arXiv preprint arXiv:2007.13302*.
- Loiola, E. M., de Abreu, N. M. M., Boaventura-Netto, P. O., Hahn, P., and Querido, T. (2007). A survey for the quadratic assignment problem. *European journal of operational research*, 176(2):657–690.
- Lugosi, G. (2002). Pattern classification and learning theory. In *Principles of nonparametric learning*, pages 1–56. Springer.
- Macchi, O. (1975). The coincidence approach to stochastic point processes. *Advances in Applied Probability*, 7(1):83–122.
- Manski, C. F. (2004). Statistical treatment rules for heterogeneous populations. *Econometrica*, 72(4):1221–1246.
- Manski, C. F. (2010). Vaccination with partial knowledge of external effectiveness. *Proceedings of the National Academy of Sciences*, 107(9):3953–3960.
- Manski, C. F. (2013). Identification of treatment response with social interactions. *The Econometrics Journal*, 16(1):S1–S23.
- Manski, C. F. (2017). Mandating vaccination with unknown indirect effects. *Journal of Public Economic Theory*, 19(3):603–619.

- Manski, C. F. (2019). Treatment choice with trial data: statistical decision theory should supplant hypothesis testing. *The American Statistician*, 73(sup1):296–304.
- Manski, C. F. and Molinari, F. (2020). Estimating the covid-19 infection rate: Anatomy of an inference problem. *Journal of Econometrics*.
- Mbakop, E. and Tabord-Meehan, M. (2016). Model selection for treatment choice: Penalized welfare maximization. *arXiv preprint arXiv:1609.03167*.
- Miao, Y. (2010). Concentration inequality of maximum likelihood estimator. *Applied mathematics letters*, 23(10):1305–1309.
- Mirzasoaleiman, B., Badanidiyuru, A., Karbasi, A., Vondrák, J., and Krause, A. (2014). Lazier than lazy greedy. *arXiv preprint arXiv:1409.7938*.
- Mirzasoaleiman, B., Karbasi, A., Sarkar, R., and Krause, A. (2013). Distributed submodular maximization: Identifying representative elements in massive data. In *Advances in Neural Information Processing Systems*, pages 2049–2057.
- Narayanan, H. (1997). *Submodular functions and electrical networks*, volume 54. Elsevier.
- Nåsell, I. (1996). The quasi-stationary distribution of the closed endemic sis model. *Advances in Applied Probability*, pages 895–932.
- Nemhauser, G. L., Wolsey, L. A., and Fisher, M. L. (1978). An analysis of approximations for maximizing submodular set functions—i. *Mathematical programming*, 14(1):265–294.
- Pastor-Satorras, R. and Vespignani, A. (2002). Immunization of complex networks. *Physical review E*, 65(3):036104.
- Pesaran, H. and Yang, C. F. (2020). Matching theory and evidence on covid-19 using a stochastic model of epidemics on networks. *IAAE Webinar*.
- Rubin, D. B. (1974). Estimating causal effects of treatments in randomized and nonrandomized studies. *Journal of educational Psychology*, 66(5):688.
- Sakaguchi, S. (2019). Estimating optimal dynamic treatment assignment rules under intertemporal budget constraints. *working paper*.

- Sävje, F., Aronow, P. M., and Hudgens, M. G. (2017). Average treatment effects in the presence of unknown interference. *arXiv preprint arXiv:1711.06399*.
- Stock, J. H. (2020). Data gaps and the policy response to the novel coronavirus. Technical report, National Bureau of Economic Research.
- Stoye, J. (2009). Minimax regret treatment choice with finite samples. *Journal of Econometrics*, 151(1):70–81.
- Stoye, J. (2012). Minimax regret treatment choice with covariates or with limited validity of experiments. *Journal of Econometrics*, 166(1):138–156.
- Tetenov, A. (2012). Statistical treatment choice based on asymmetric minimax regret criteria. *Journal of Econometrics*, 166(1):157–165.
- Vazquez-Bare, G. (2020). Causal spillover effects using instrumental variables. *arXiv preprint arXiv:2003.06023*.
- Viviano, D. (2019). Policy targeting under network interference. *arXiv preprint arXiv:1906.10258*.
- WHO et al. (2020a). Draft landscape of covid-19 candidate vaccines. *World*.
- WHO et al. (2020b). Fair allocation mechanism for covid-19 vaccines through the covax facility. *World*.
- WHO et al. (2020c). A global framework to ensure equitable and fair allocation of covid-19 products and potential implications for covid-19 vaccines. june 18, 2020.
- Zhao, Y., Zeng, D., Rush, A. J., and Kosorok, M. R. (2012). Estimating individualized treatment rules using outcome weighted learning. *Journal of the American Statistical Association*, 107(499):1106–1118.
- Zhao, Y.-Q., Zeng, D., Laber, E. B., and Kosorok, M. R. (2015). New statistical learning methods for estimating optimal dynamic treatment regimes. *Journal of the American Statistical Association*, 110(510):583–598.
- Zhou, Z., Athey, S., and Wager, S. (2018). Offline multi-action policy learning: Generalization and optimization. *arXiv preprint arXiv:1810.04778*.

Appendix A The Transmission Term

Consider a susceptible individual i with κ_s contracts which depends on his own characteristics at each period. Of these, a fraction $\sum_{j \in N_i} I_j(1 - v_j)a_j/|N_i|$ are contracts with infected neighbors from group 1, and a fraction $\sum_{j \in N_i} I_j(1 - v_j)b_j/|N_i|$ are contracts with infected neighbors from group 2. If we define c_{ij} as the probability of successful disease transmission for each contact, then $1 - c_{sk}$ is the probability that transmission between group s and group k does not take place. Therefore, we have the probability that a unit i is not infected at one time period:

$$\begin{aligned}
 1 - q_i &= (1 - c_{11}) \frac{\kappa_1 \sum_{j \in N_i} I_j(1 - v_j)a_j a_i}{|N_i|} \\
 &\cdot (1 - c_{12}) \frac{\kappa_1 \sum_{j \in N_i} I_j(1 - v_j)b_j a_i}{|N_i|} \\
 &\cdot (1 - c_{21}) \frac{\kappa_2 \sum_{j \in N_i} I_j(1 - v_j)a_j b_i}{|N_i|} \\
 &\cdot (1 - c_{22}) \frac{\kappa_2 \sum_{j \in N_i} I_j(1 - v_j)b_j b_i}{|N_i|}
 \end{aligned} \tag{44}$$

We now define $\beta_{sk} = -\kappa_s \log(1 - c_{sk})$ and plug it into the expression for $1 - q_i$, which allows us to rewrite above equation as:

$$q_i = 1 - e^{-z}, \tag{45}$$

where

$$\begin{aligned}
 z &= \frac{\beta_{11}}{|N_i|} \sum_{j \in N_i} I_j(1 - v_j)a_j a_i \\
 &+ \frac{\beta_{12}}{|N_i|} \sum_{j \in N_i} I_j(1 - v_j)b_j a_i \\
 &+ \frac{\beta_{21}}{|N_i|} \sum_{j \in N_i} I_j(1 - v_j)a_j b_i \\
 &+ \frac{\beta_{22}}{|N_i|} \sum_{j \in N_i} I_j(1 - v_j)b_j b_i.
 \end{aligned} \tag{46}$$

Recalling that $e^x = 1 + x + \frac{x^2}{2} + \frac{x^3}{3} + \dots$, we now have the probability of infection at each time period as

$$q_i = z \tag{47}$$

Appendix B Lemmas

B.1 Preliminary Lemma

In this section we collect a set of lemmas from past literature that we used in our proofs.

Lemma B.1 (Proposition 6.3 [Bach \(2011\)](#)). *Let $Q \in \mathbb{R}^{p \times p}$ and $q \in \mathbb{R}^{p \times 1}$. Then the function $F \mapsto q^\top \mathbf{1}_A + \frac{1}{2} \mathbf{1}_A^\top Q \mathbf{1}_A$ is submodular if and only if all off-diagonal elements of Q are non-positive.*

Lemma B.2 (Theorem 2.2 [Cunningham \(1985\)](#)). *Function F is a cut function if and only if: For any three disjoint subsets A, B, C of S ,*

$$F(A \cup B \cup C) = F(A \cup B) + F(A \cup C) + F(B \cup C) - F(A) - F(B) - F(C) + F(\emptyset)$$

The following lemmas are some common techniques that are often used in statistical learning literature, as reviewed in [Lugosi \(2002\)](#).

Lemma B.3 (Hoeffding's inequality [Hoeffding \(1994\)](#)). *Let X_1, \dots, X_n be independent bounded random variables such that X_i falls in the interval $[a_i, b_i]$ with probability one. Denote their sum by $S_n = \sum_{i=1}^n X_i$. Then for any $\epsilon > 0$ we have*

$$\mathbb{P}\{S_n - \mathbb{E} S_n \geq \epsilon\} \leq e^{-2\epsilon^2 / \sum_{i=1}^n (b_i - a_i)^2}$$

and

$$\mathbb{P}\{S_n - \mathbb{E} S_n \leq -\epsilon\} \leq e^{-2\epsilon^2 / \sum_{i=1}^n (b_i - a_i)^2}$$

B.2 Proof of Lemma 4.1

Let $\hat{W} \in \mathbb{R}^{N \times N}$ and $\hat{C} \in \mathbb{R}^N$. Then the function $F_n: \mathbf{V} \mathbf{v}^\top \hat{W} \mathbf{v} + \hat{C}^\top \mathbf{v} - \mathbf{1}_{N \times 1}^\top \hat{W} \mathbf{v} - \mathbf{v}^\top \hat{W} \mathbf{1}_{N \times 1}$ is submodular if and only if $\hat{w}_{ij} \leq 0 \forall i \neq j$.

Proof. The first step is to show our objective function is a cut function based on Lemma B.2. In our case, simply consider three individuals $i, j, k \subseteq \mathcal{N}$

$$\begin{aligned}
F_n(i \cup j \cup k) &= \hat{w}_{ii} + \hat{w}_{jj} + \hat{w}_{kk} + 2\hat{w}_{ij} + 2\hat{w}_{ik} + 2\hat{w}_{jk} + \hat{c}_i + \hat{c}_j + \hat{c}_k \\
&\quad - \sum_{m=1}^N \hat{w}_{mi}v_i - \sum_{m=1}^N \hat{w}_{mj}v_j - \sum_{m=1}^N \hat{w}_{mk}v_k \\
&\quad - \sum_{m=1}^N \hat{w}_{im}v_i - \sum_{m=1}^N \hat{w}_{jm}v_j - \sum_{m=1}^N \hat{w}_{km}v_m
\end{aligned} \tag{48}$$

$$F_n(i \cup j) = \hat{w}_{ii} + \hat{w}_{jj} + 2\hat{w}_{ij} + \hat{c}_i + \hat{c}_j - \sum_{m=1}^N \hat{w}_{mi}v_i - \sum_{m=1}^N \hat{w}_{mj}v_j - \sum_{m=1}^N \hat{w}_{im}v_i - \sum_{m=1}^N \hat{w}_{jm}v_j \tag{49}$$

$$F_n(i \cup k) = \hat{w}_{ii} + \hat{w}_{kk} + 2\hat{w}_{ik} + \hat{c}_i + \hat{c}_k - \sum_{m=1}^N \hat{w}_{mi}v_i - \sum_{m=1}^N \hat{w}_{mk}v_k - \sum_{m=1}^N \hat{w}_{im}v_i - \sum_{m=1}^N \hat{w}_{km}v_m \tag{50}$$

$$F_n(j \cup k) = \hat{w}_{jj} + \hat{w}_{kk} + 2\hat{w}_{jk} + \hat{c}_j + \hat{c}_k - \sum_{m=1}^N \hat{w}_{mj}v_j - \sum_{m=1}^N \hat{w}_{mk}v_k - \sum_{m=1}^N \hat{w}_{jm}v_j - \sum_{m=1}^N \hat{w}_{km}v_m \tag{51}$$

$$F_n(i) = \hat{w}_{ii} + \hat{c}_i - \sum_{m=1}^N \hat{w}_{mi}v_i - \sum_{m=1}^N \hat{w}_{im}v_i \tag{52}$$

$$F_n(j) = \hat{w}_{jj} + \hat{c}_j - \sum_{m=1}^N \hat{w}_{mj}v_j - \sum_{m=1}^N \hat{w}_{jm}v_j \tag{53}$$

$$F_n(k) = \hat{w}_{kk} + \hat{c}_k - \sum_{m=1}^N \hat{w}_{mk}v_k - \sum_{m=1}^N \hat{w}_{km}v_m \tag{54}$$

$$F_n(\emptyset) = 0 \tag{55}$$

$$\Rightarrow F_n(i \cup j \cup k) = F_n(i \cup j) + F_n(i \cup k) + F_n(j \cup k) - F_n(i) - F_n(j) - F_n(k) + F_n(\emptyset) \quad (56)$$

Now, We have shown that $F_n(V)$ is a cut function. The next step is to find the sufficient and necessary condition for submodularity of the cut function. Lemma B.1 indicates for any cut function which can be written as a quadratic function plus a linear part, it is submodular if and only if all off-diagonal elements of weighting matrix is non-positive. That requires $\hat{w}_{ij} \leq 0, \forall i \neq j$. \square

B.3 Proof of Lemma 5.1

Under Assumption 2.1, 2.2, and 5.1, we have

$$\mathbb{E}_{P^n} |\hat{w}_{ij} - w_{ij}| \leq \sqrt{\frac{1 + \log(2)}{2n}} \frac{A_{ij}}{N} \quad \mathbb{E}_{P^n} |\hat{c}_i - c_i| \leq \sqrt{\frac{1 + \log(2)}{2n}} \frac{I_i}{N} \quad (57)$$

Proof. We first prove the upper bound of $\mathbb{E}_{P^n} |\hat{w}_{ij} - w_{ij}|$

$$\begin{aligned} \hat{w}_{ij} - w_{ij} = \frac{1}{|N_i|N} & \left[-(\hat{\beta}_{11} - \beta_{11})a_i S_i A_{ij} a_j I_j - (\hat{\beta}_{12} - \beta_{12})a_i S_i A_{ij} b_j I_j \right. \\ & \left. - (\hat{\beta}_{21} - \beta_{21})b_i S_i A_{ij} a_j I_j - (\hat{\beta}_{22} - \beta_{22})b_i S_i A_{ij} b_j I_j \right] \end{aligned} \quad (58)$$

If we take absolute value and expectation at each side, by triangle inequality, we can get

$$\begin{aligned} \mathbb{E}_{P^n} |\hat{w}_{ij} - w_{ij}| &= \frac{1}{|N_i|N} \mathbb{E}_{P^n} \left| (\hat{\beta}_{11} - \beta_{11})a_i S_i A_{ij} a_j I_j + (\hat{\beta}_{12} - \beta_{12})a_i S_i A_{ij} b_j I_j \right. \\ & \quad \left. + (\hat{\beta}_{21} - \beta_{21})b_i S_i A_{ij} a_j I_j + (\hat{\beta}_{22} - \beta_{22})b_i S_i A_{ij} b_j I_j \right| \\ &\leq \frac{1}{|N_i|N} \mathbb{E}_{P^n} \left| \hat{\beta}_{11} - \beta_{11} \right| a_i S_i A_{ij} a_j I_j + \frac{1}{|N_i|N} \mathbb{E}_{P^n} \left| \hat{\beta}_{12} - \beta_{12} \right| a_i S_i A_{ij} b_j I_j \\ & \quad + \frac{1}{|N_i|N} \mathbb{E}_{P^n} \left| \hat{\beta}_{21} - \beta_{21} \right| b_i S_i A_{ij} a_j I_j + \frac{1}{|N_i|N} \mathbb{E}_{P^n} \left| \hat{\beta}_{22} - \beta_{22} \right| b_i S_i A_{ij} b_j I_j \end{aligned} \quad (59)$$

Since β_{sk} is the effective contact rate of the disease between group s and k , it is naturally

bounded by $[0, 1]$. We can apply lemma B.3 to get the upper bound of each component:

$$\mathbb{P}\left\{\left|\hat{\beta}_{11} - \beta_{11}\right| \geq \epsilon\right\} \leq 2e^{-2n\epsilon^2} \quad (60)$$

$$\mathbb{P}\left\{\left|\hat{\beta}_{12} - \beta_{12}\right| \geq \epsilon\right\} \leq 2e^{-2n\epsilon^2} \quad (61)$$

$$\mathbb{P}\left\{\left|\hat{\beta}_{21} - \beta_{21}\right| \geq \epsilon\right\} \leq 2e^{-2n\epsilon^2} \quad (62)$$

$$\mathbb{P}\left\{\left|\hat{\beta}_{22} - \beta_{22}\right| \geq \epsilon\right\} \leq 2e^{-2n\epsilon^2} \quad (63)$$

We can find one general tail bound for all $\beta = \beta_{11}, \beta_{12}, \beta_{21}, \beta_{22}$, which is stated in the assumption 5.1.

$$\mathbb{P}\left\{\left|\hat{\beta} - \beta\right| \geq \epsilon\right\} \leq 2e^{-2n\epsilon^2} \quad (64)$$

Now we can bound the $\mathbb{E}(|\hat{\beta} - \beta|)$. Recall that for any nonnegative random variable Y , $\mathbb{E}(Y) = \int_0^\infty \mathbb{P}(Y \geq t)dt$. Hence, for any $a > 0$,

$$\begin{aligned} \mathbb{E}(|\hat{\beta} - \beta|^2) &= \int_0^\infty \mathbb{P}(|\hat{\beta} - \beta|^2 \geq t)dt \\ &= \int_0^a \mathbb{P}(|\hat{\beta} - \beta|^2 \geq t)dt + \int_a^\infty \mathbb{P}(|\hat{\beta} - \beta|^2 \geq t)dt \\ &\leq a + \int_a^\infty \mathbb{P}(|\hat{\beta} - \beta|^2 \geq t)dt \end{aligned} \quad (65)$$

Equation 64 implies that $\mathbb{P}(|\hat{\beta} - \beta| \geq \sqrt{t}) \leq 2e^{-2nt}$. Hence,

$$\begin{aligned} \mathbb{E}(|\hat{\beta} - \beta|^2) &\leq a + \int_a^\infty \mathbb{P}(|\hat{\beta} - \beta|^2 \geq t)dt \\ &= a + \int_a^\infty \mathbb{P}(|\hat{\beta} - \beta| \geq \sqrt{t})dt \\ &\leq a + 2 \int_a^\infty e^{-2nt} dt \\ &= a + \frac{e^{-2na}}{n} \end{aligned} \quad (66)$$

Set $a = \log(2)/(2n)$ and we have

$$\mathbb{E}(|\hat{\beta} - \beta|^2) \leq \frac{\log(2)}{2n} + \frac{1}{2n} = \frac{1 + \log(2)}{2n} \quad (67)$$

Therefore, we have

$$\mathbb{E}(|\hat{\beta} - \beta|) \leq \sqrt{\mathbb{E}(|\hat{\beta} - \beta|^2)} \leq \sqrt{\frac{1 + \log(2)}{2n}} \quad (68)$$

Plug that upper bound back to equation 59, we get

$$\begin{aligned} \mathbb{E}|\hat{w}_{ij} - w_{ij}| &\leq \sqrt{\frac{1 + \log(2)}{2n}} (a_i S_i A_{ij} a_j I_j + a_i S_i A_{ij} b_j I_j + b_i S_i A_{ij} a_j I_j + b_i S_i A_{ij} b_j I_j) \frac{1}{|N_i| N} \\ &(\because |N_i| \geq 1 \text{ by treating } 0 \text{ neighbor as equal to } 1) \\ &= \sqrt{\frac{1 + \log(2)}{2n}} \frac{A_{ij}}{N} \end{aligned} \quad (69)$$

The idea of proof the upper bound for $E_{P^n}|\hat{c}_i - c_i|$ is exactly same,

$$\hat{c}_i - c_i = -(\hat{\gamma}_1 - \gamma_1)a_i I_i / N - (\hat{\gamma}_2 - \gamma_2)b_i I_i / N. \quad (70)$$

Take absolute value and expectation at both side,

$$\begin{aligned} \mathbb{E}|\hat{c}_i - c_i| &= \mathbb{E}|(\hat{\gamma}_1 - \gamma_1)a_i I_i / N + (\hat{\gamma}_2 - \gamma_2)b_i I_i / N| \\ &\leq \mathbb{E}|\hat{\gamma}_1 - \gamma_1| a_i I_i / N + \mathbb{E}|\hat{\gamma}_2 - \gamma_2| b_i I_i / N. \end{aligned} \quad (71)$$

With the same idea of β , γ is also bounded by $[0, 1]$. By using lemma B.3, we could get

$$\mathbb{E}|\hat{\gamma} - \gamma| \leq \sqrt{\frac{1 + \log(2)}{2n}} \quad \forall \hat{\gamma} = \hat{\gamma}_1, \hat{\gamma}_2 \quad (72)$$

Plug that upper bound back to equation 71, we get

$$\begin{aligned} \mathbb{E}|\hat{c}_i - c_i| &\leq \sqrt{\frac{1 + \log(2)}{2n}} (a_i I_i + b_i I_i) / N \\ &= \sqrt{\frac{1 + \log(2)}{2n}} \frac{I_i}{N} \end{aligned} \quad (73)$$

□

Appendix C Proofs for Theorems

C.1 Proof of Theorem 4.1

The objective function $F_n(V)$ is a non-decreasing submodular function for any adjacency matrix, covariate values, and values of parameter estimates.

Proof. Recall

$$F_n(V) = \mathbf{v}^\top \hat{W} \mathbf{v} + \hat{C}^\top \mathbf{v} - \mathbf{1}_{N \times 1}^\top \hat{W} \mathbf{v} - \mathbf{v}^\top \hat{W} \mathbf{1}_{N \times 1}. \quad (74)$$

In here, \mathbf{V} is the vector of integers. Let us first look at this function in the continuous case. Imagine now we have a vector $\tilde{\mathbf{V}}$ which has all elements are continuous. Then, this function becomes:

$$\tilde{F}_n(V) = \tilde{\mathbf{v}}^\top \hat{W} \tilde{\mathbf{v}} + \hat{C}^\top \tilde{\mathbf{v}} - \mathbf{1}_{N \times 1}^\top \hat{W} \tilde{\mathbf{v}} - \tilde{\mathbf{v}}^\top \hat{W} \mathbf{1}_{N \times 1}. \quad (75)$$

We can write the derivative of $F_n(V)$ with respect to $\tilde{\mathbf{V}}$:

$$\begin{aligned} \frac{\partial \tilde{F}_n(V)}{\partial \tilde{\mathbf{v}}} &= \tilde{\mathbf{v}}^\top \hat{W}^\top + \tilde{\mathbf{v}}^\top \hat{W} + \hat{C}^\top - \mathbf{1}_{N \times 1}^\top \hat{W} - \mathbf{1}_{N \times 1}^\top \hat{W}^\top \\ &= \underbrace{(\tilde{\mathbf{v}}^\top - \mathbf{1}_{N \times 1}^\top)}_{\leq 0} \underbrace{\hat{W}^\top}_{\leq 0} + \underbrace{(\tilde{\mathbf{v}}^\top - \mathbf{1}_{N \times 1}^\top)}_{\leq 0} \underbrace{\hat{W}}_{\leq 0} + \underbrace{\hat{C}^\top}_{\geq 0} \\ &\geq 0 \end{aligned} \quad (76)$$

Given all the elements in $\frac{\partial \tilde{F}_n(V)}{\partial \tilde{\mathbf{v}}}$ are non-negative, this property should also hold under integer case (i.e. $\frac{\partial F_n(V)}{\partial \mathbf{v}} \geq 0$). Recall the definition of non-decreasing set function ([Bellstedt and Dathe, 1992](#)):

$$F(\mathcal{N}) = \{r: 2^{\mathcal{N}} \rightarrow \mathbb{R}; I \subseteq J \rightarrow r(I) \leq r(J); \forall I \subseteq J \subseteq \mathcal{N}\}. \quad (77)$$

Therefore, if we can show $F_n(I) \leq F_n(J); \forall I \subseteq J \subseteq \mathcal{N}$, then our objective function $F_n(V)$ is non-decreasing. Given $\frac{\partial F_n(V)}{\partial \mathbf{v}}$ is non-negative for each element, we can say for any

$I \subseteq J \subseteq \mathcal{N}$, $F_n(J) \geq F_n(I)$. Therefore, $F_n(V)$ is non-decreasing set function. Combining with lemma 4.1, we finish the proof. \square

C.2 Proof of Theorem 5.1

Let $N_M = \max_{i \in \mathcal{N}} |N_i|$, and N_I be the total number of infected units. Under Assumptions 2.1, 2.2, and 5.1, we have

$$\mathbb{E}_{P^n} \left[F(V^*) - F(\hat{V}) \right] \leq \bar{C} \cdot \frac{3dN_M + \min\{N_I, d\}}{N} \sqrt{\frac{1}{n}} + \frac{1}{e} F(V^*), \quad (78)$$

where \bar{C} is a universal constant and d is the number of available vaccines.

Proof.

$$\begin{aligned} \mathbb{E}_{P^n} \left[\sup_{V \in \mathcal{V}_d} |F_n(V) - F(V)| \right] &\leq \mathbb{E}_{P^n} \left[\sup_{V \in \mathcal{V}_d} \mathbf{v}^\top \left| \hat{W} - W \right| \mathbf{v} \right] + \mathbb{E}_{P^n} \left[\sup_{V \in \mathcal{V}_d} \left| \hat{C}^\top - C^\top \right| \mathbf{v} \right] \\ &\quad + \mathbb{E}_{P^n} \left[\sup_{V \in \mathcal{V}_d} \mathbf{1}_{N \times 1}^\top \left| \hat{W} - W \right| \mathbf{v} \right] + \mathbb{E}_{P^n} \left[\sup_{V \in \mathcal{V}_d} \mathbf{v}^\top \left| \hat{W} - W \right| \mathbf{1}_{N \times 1} \right] \\ &= \sup_{V \in \mathcal{V}_d} \mathbf{v}^\top \mathbb{E}_{P^n} \left| \hat{W} - W \right| \mathbf{v} + \sup_{V \in \mathcal{V}_d} \mathbb{E}_{P^n} \left| \hat{C}^\top - C^\top \right| \mathbf{v} \\ &\quad + \sup_{V \in \mathcal{V}_d} \mathbf{1}_{N \times 1}^\top \mathbb{E}_{P^n} \left| \hat{W} - W \right| \mathbf{v} + \sup_{V \in \mathcal{V}_d} \mathbf{v}^\top \mathbb{E}_{P^n} \left| \hat{W} - W \right| \mathbf{1}_{N \times 1} \end{aligned} \quad (79)$$

From equation 79, $\mathbb{E}_{P^n} \left[\sup_{V \in \mathcal{V}_d} |F_n(V) - F(V)| \right]$ can be decomposed into four components. Since \mathbf{v} only contains $\{0, 1\}$ and the absolute value must be non-negative, the V that maximize each component under capacity constraint must choose the units with higher number of edges compare to the non-selected units. We define the maximum number of edges for each unit as N_M . Hence, the number of edges for selected units must be lower or equal to N_M . Next, we look at each term in equation 79 separately. Using Lemma 5.1, the first term is bounded as:

$$\begin{aligned}
\sup_{V \in \mathcal{V}_d} \mathbf{v}^\top \mathbb{E}_{P^n} \left| \hat{W} - W \right| \mathbf{v} &\leq \sup_{V \in \mathcal{V}_d} \sqrt{\frac{1 + \log(2)}{2n}} \frac{\sum_{i \in V} \sum_{j \in V} A_{ij}}{N} \\
&\leq \sqrt{\frac{1 + \log(2)}{2n}} \frac{\sum_{i \in V} N_M}{N} \\
&\left(\because \sum_{j \in V} A_{ij} \leq N_M \quad \forall i \in \mathcal{N} \right) \\
&\leq \sqrt{\frac{1 + \log(2)}{2n}} \frac{dN_M}{N}.
\end{aligned} \tag{80}$$

The second term is bounded as:

$$\begin{aligned}
\sup_{V \in \mathcal{V}_d} \mathbb{E}_{P^n} \left| \hat{C}^\top - C^\top \right| \mathbf{v} &\leq \sup_{V \in \mathcal{V}_d} \sqrt{\frac{1 + \log(2)}{2n}} \frac{\sum_{i \in V} I_i}{N} \\
&\leq \sqrt{\frac{1 + \log(2)}{2n}} \frac{\min\{N_I, d\}}{N}.
\end{aligned} \tag{81}$$

The third term is bounded as:

$$\begin{aligned}
\sup_{V \in \mathcal{V}_d} \mathbf{1}_{N \times 1}^\top \mathbb{E}_{P^n} \left| \hat{W} - W \right| \mathbf{v} &\leq \sup_{V \in \mathcal{V}_d} \sqrt{\frac{1 + \log(2)}{2n}} \frac{\sum_{i \in \mathcal{N}} \sum_{j \in V} A_{ij}}{N} \\
&\leq \sqrt{\frac{1 + \log(2)}{2n}} \frac{\sum_{j \in V} N_M}{N} \\
&= \sqrt{\frac{1 + \log(2)}{2n}} \frac{dN_M}{N}.
\end{aligned} \tag{82}$$

The fourth term is bounded as:

$$\begin{aligned}
\sup_{V \in \mathcal{V}_d} \mathbf{v}^\top \mathbb{E}_{P^n} \left| \hat{W} - W \right| \mathbf{1}_{N \times 1} &\leq \sup_{V \in \mathcal{V}_d} \sqrt{\frac{1 + \log(2)}{2n}} \frac{\sum_{i \in V} \sum_{j \in \mathcal{N}} A_{ij}}{N} \\
&\leq \sqrt{\frac{1 + \log(2)}{2n}} \frac{\sum_{i \in V} N_M}{N} \\
&= \sqrt{\frac{1 + \log(2)}{2n}} \frac{dN_M}{N}.
\end{aligned} \tag{83}$$

Combining the bound of four terms together, we could get

$$\begin{aligned} \mathbb{E}_{\mathcal{P}^n} \left[\sup_{V \in \mathcal{V}_d} |F_n(V) - F(V)| \right] &\leq 3\sqrt{\frac{1 + \log(2)}{2n}} \frac{dN_M}{N} + \sqrt{\frac{1 + \log(2)}{2n}} \frac{\min\{N_I, d\}}{N} \\ &= \frac{3dN_M + \min\{N_I, d\}}{N} \sqrt{\frac{1 + \log(2)}{2n}}. \end{aligned} \quad (84)$$

Therefore, we have

$$\mathbb{E}_{\mathcal{P}^n} [F(V^*) - F(\hat{V})] \leq \left(2 + \frac{1}{e}\right) \frac{3dN_M + \min\{N_I, d\}}{N} \sqrt{\frac{1 + \log(2)}{2n}} + \frac{1}{e} F(V^*). \quad (85)$$

□